Ski Jump Launch Trainer

December 10th, 2025

Biomedical Engineering 200/300

Section 303

Client: Dr. Azam Ahmed

Dept. of Neurological Surgery and Radiology, UW Health

Advisor: Dr. Randy Bartels

Dept. of Biomedical Engineering, UW-Madison

Team Members:
Kenneth Sun (Leader) | kksun2@wisc.edu
Caleb White (BSAC) | cfwhite@wisc.edu
Presley Stellflue (Communicator) | pstellflue@wisc.edu
Matthew Niemuth (BWIG) | mniemuth@wisc.edu
Sarah Kong (BPAG) | smkong@wisc.edu

Abstract

Ski jumping performance is, through tradition, subjectively evaluated through coach and judge observation and scoring. Despite the heavy technical demands intrinsic to the sport, the methodology of improvement and success lacks any level of technical analysis or quantitative reasoning. This creates a clear need for the development of a quantitative data collection system that gives athletes clearer, more practical feedback, that will help them refine their skills more consistently. Current technologies such as commercial force insoles, IMUs, and markerless motion capture provide isolated measurements but are too costly, not applicable in ski jump settings, and not tailored to real-world use respectively. This project looks to develop an integrated, low-cost data collection training system capable of quantifying various biomechanical variables for coaches to analyze, allowing for the development of data driven feedback for their youth athletes.

The final system combined custom 3D-printed force-sensing insoles with Velostat, a 6-DOF inertial measurement unit, a microcontroller-based wireless data interface pipeline, and 2D motion analysis through Kinovea. Through calibration and system testing, results indicated the potential of the combined system's ability to provide clear organized data on force production, weight distribution, and joint kinematics in a manner suitable for quantitative athlete feedback. Although variability in Velostat force output and 2D marker drift introduced minor error, the collected data still provides meaningful trends that can separate and compare the quality of various jumps. This project establishes a foundation for data-based coaching in youth ski jumping, and provides the tools required to build long-term quantitative reasoning behind successful ski jump performance. The system will push ski jumping towards a modern, data-driven training approach, much like the technological progress seen in other sports and enable the creation of standardized performance markers, promoting fairer coaching practices, and supporting long-term metric databases that can aid athletes and teams at every level.

Table of Contents

Introduction

Motivation

Ski jumping first began in Norway in the 19th century and has increased in popularity around the world, becoming a fan favorite sport at the Winter Olympic Games [1]. Video analysis-based coaching has also grown in popularity as, regardless of endeavor, it provides athletes with the opportunity to observe their physical performance from an outside perspective, providing insight into the form and approach being taken [2]. Furthermore, a focus on quantitative video analysis, emphasizing key Newtonian biomechanical metrics, has emerged as a recent advancement that has been enabled by improvements in high-speed video cameras and artificial intelligence-based motion tracking [3]. Unfortunately, the use of video analysis-based feedback has not been widely implemented in ski jumping compared to other sports such as track and field or baseball [4]. Implementing this more quantitative approach will be much more useful compared to the old qualitative approach where any feedback provided by coaches or judges is based on subjective perception of form and timing. In a sport that is very dependent on form and approach, combined with its unique complex physics basis, the need for a quantitative-based visual learning system that tracks specific performance metrics and provides immediate feedback for areas of refinement is apparent. This feedback should be rooted in quantitative data that demonstrates a high correlation with jump quality. This system has the potential to not only provide coaches access to data-driven feedback but also enhance athlete safety by identifying poor takeoff mechanics while establishing more training rigor to further develop a growing sport.

Current Methods

The current scope of ski jump training video analysis is based on a subjective and qualitative assessment. More specifically, formal quantitative assessments of ski jump performance have yet to be implemented as a traditional coaching tool [5]. Already in limited supply, most of the domain of published quantitative ski jump analysis relate to investigative explorations of sensor and data tracking in intense environments without regard to how the data collected from the sensors could be used for direct feedback. For example, the combined use of a differential Global Navigation Satellite System (dGNSS) and a markerless video-based pose estimation system in a Norwegian study allowed the collection of key body angle and force metrics. However, this data was used to prove equivalency between the two tracking methods themselves, rather than any specific investigation of a physics-based hypothesis that could be filtered into specific feedback for athletes [4].

Figure 1: Angle analysis from Markerless Video-Based Pose Estimation recording demonstrating the application of post processing angle determination from the sagittal plane [4].

For force plate or pressure data collection, modern pressure tracking insole systems that sectionalize major parts of the foot are mostly commercial products. Several of these products have been used in ski jumping-related investigations, including the aforementioned dGNSS study; however, they are not limited to this specific application. These insoles provide insight into weight distribution and reaction force data created by the specific movements being performed by the athlete [6]. In a study focused on a full-body inertial measurement unit (IMU) analysis of ski jumpers, these force insoles can be used in conjunction with other forms of data tracking to provide supporting data for certain observed results. Again, the purpose of the study being referenced was to evaluate the specific measurement system to be further applied to further dynamic analysis, not an improving ski jumping results specific inquiry [7].
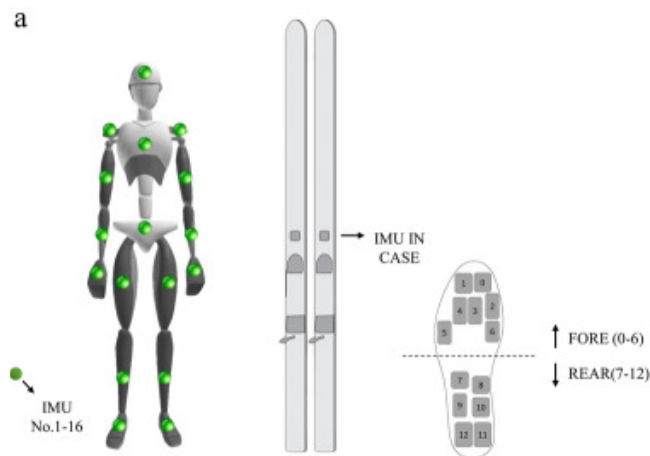

Figure 2: IMU and force insole sensor distribution on the body, skis, and boots of the athlete [7].

Problem Statement

This project aims to develop and prototype a comprehensive training system that collects biomechanical data during the in-run and take-off portions of a ski jump that allows coaches to give quantitative based feedback to assist youth ski jumpers in improving their skills. The system will integrate 2D motion analysis, force plates, and inertial measurement units to capture the determined biomechanical data, such as body joint angles and ground reaction forces. Production of this system will give the coaches at Blackhawk ski club the resources and tools to quantitatively characterize individual jumps and help build specific proportional relationships between these biomechanical variables and performance outcomes (qualitative scores). Establishing these relationships will alter the format of ski jump training and will give access to targeted, evidence-based feedback that can guide youth ski jumper training to optimize performance and bridge the gap between amateur and professional performance.

Background

Biomechanics of Ski Jumping

Ski jumping is a highly technical sport that rewards points based on jump distance and style. There are 5 phases in ski jumping: in-run, takeoff, early flight, stable flight, and landing. The first 3 phases are important for analyzing biomechanical metrics that will ultimately help the jumper improve technique as there is proven correlation between good form within these phases with higher velocity and farther jump distance [8]. These phases in particular involve the transfer of mechanical energy from the lower body to the skier's center of mass where coordinated muscle activation generates that explosive impulse needed to convert horizontal velocity into vertical lift at takeoff. Precise coordination of the lower-body musculature is essential, as the stretch-shortening cycle in the quadriceps and calf muscles boosts force production and contributes to a more explosive lift-off. During the early flight stages, judges focus on the symmetry of the ski-opening angle, torso orientation, knee and ankle flexion, and the positioning of the arms. Effective coordination between the ankle, knee, and hip joints ensures smoother transitions into flight and greater aerodynamic efficiency. Maintaining an optimal ski-opening angle and ankle angles enhances the lift-to-drag ratio [9]. Additionally, analyzing body composition and angles during the in-run phase is crucial for maximizing aerodynamics. Specifically, the torso and thigh attack angles, as well as the ankle joint and hip joint abduction angles, have the most influence on drag. Small adjustments in the torso angle produce larger changes in drag than equivalent changes at the lower body angles [10]. A smaller angle between the torso, hip joint, and thigh, will allow for more air-time and greater flight distance. As shown in the diagram below, the angle, beta, represents the flexion of the feet after takeoff and the angle, alpha, represents the torso/hip angle. When these two values are minimized, the lift ratio increases. In ski jumping, these angles are not visibly measured and the scoring of a ski jump is based on distance and style, rendering it a qualitative sport.
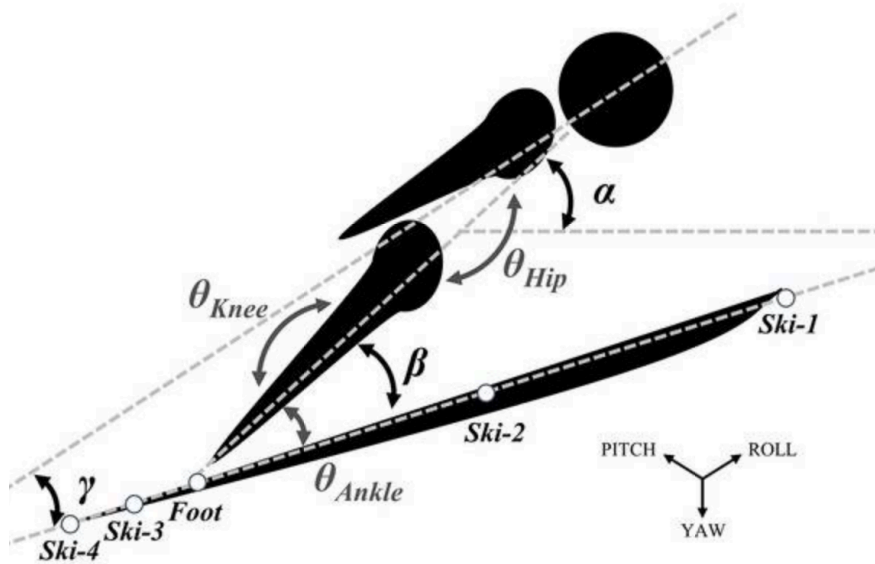
Figure 3: Diagram of critical angles during the flight phase of a ski jump.

Scoring

Ski jumping incorporates two aspects to judge the success of a jump: K-score and style points. For distance, ski jumping incorporates a K-score metric that involves a K-point which is the spot where the ski hill flattens out. Landing on this K-point gives a set amount of points, with every extra meter past the K-point adding one point and every meter before subtracting one point [11]. In terms of style points, the judges who are scoring the jump will look for a smooth transition between the in-run and the in-flight position as well as the telemark landing, which involves a graceful and staggered ski landing [11]. Together, these two main elements determine the overall quality and competitiveness of a jump.

Client

The client, Dr. Azam Ahmed, is a UW Health neurosurgeon and an associate professor in the Department of Neurological Surgery at the University of Wisconsin School of Medicine and Public Health. He has two daughters involved in youth amateur ski jumping, interested in the improvement of their technique that goes beyond coach suggestions by using quantifiable metrics to classify the quality of their jump. Both daughters have been jumping at the Blackhawk Ski Club for five years on hills that use plastic in the offseason and snow during the winter months. The client has requested a design that will allow their jumps to be analyzed into metrics quantifiable for critiques and coaching purposes.

Design Specifications

Design specifications were determined by a combination of requests from the client, literature reviews, and formal standards (see Appendix A). The system should be designed with a focus on correlating quantitative data with successful jumps to generate quantitative-based feedback that coaches can use to guide youth athletes in improving their ski jumps. The motion capture and force sensor should be used to analyze the two-second interval transition from the in-run into the takeoff phases of the jump

and then create clear points of improvement based on the acquired data. The system should be non-invasive and should have minimal impact on the athlete being tracked to ensure minimal changes in performance during data capture and normal jumps. In regards to fixed performance requirements, any force sensor recording ground reaction must be able to withstand a static load equal to 2.5 times greater than the maximum specific user weight, based on intrinsic loading requirements for general consumer recording equipment [12]. The sensors must also meet an accuracy class of at least 0.5 ,following standard recommendations of the International Vocabulary of Metrology (VIM) [13]. The system must also be able to withstand the operating environment, specifically the fluctuating and potentially harsh weather conditions in Wisconsin including 5th percentile temperatures of -23℃ (-10 ℉) and 5th percentile wind speeds of 8 m/s (18 mph), per the Wisconsin Climatology Office [14]. Representation of human models within motion capture analysis should abide by ISO/IEC 19774-2:2019 to ensure compatibility and reproducibility of data outcomes across systems. This standard includes specifics on frame rate, the use of animation of articulated characters, and specific determination of camera position [15]. Any multi-axis force platforms used in the system must be verified and calibrated per the standard ASTM F3109-22. These calibration efforts help quantify and reduce error in output signals, ensuring accurate data collection through these sensors [16]. Any human subject research must abide by OHRP and IRB protocol. This includes confirming consent of each subject with full transparency of the data being collected, the purpose of the research, and the risks of harm associated with participation. Additionally, for athletes under the age of 18, further consent from their legal guardian is required [17]. Any team members performing any level of human subject research must first be certified through human subject research training and therefore pass IRB approval and oversight [18]. Per client request, the HTML user interface and MATLAB graph analysis must be user friendly so it is easy for the coaches to understand what the data means and give feedback that helps improve the young athletes' jumps. As for the microcontroller, its housing unit must stay firmly and securely attached to the ski boot throughout the whole duration of the jump to ensure the accuracy and reliability of the data collected. If it falls off or isn't securely attached, any data collected may be invalid and not be useful for feedback to improve the athletes jump. The size of this microcontroller housing unit must also fit within a traditionally sized backpack size per DHS regulations. Specifically 0.56 m x 0.36 m x 0.23 m (see Appendix A: Preliminary Design Specifications).

Preliminary Designs

Accelerometers (IMUs)

The accelerometer (IMUs) design is based around the use of various Inertial Measurement Units that would look to provide high-frequency motion data, with a specific focus on acceleration, angular velocity, and spatial relation. Several small IMU devices would be placed on the user in several specific locations dictated by an associated machine learning software. These locations would be easy to reach, practical, and relevant locations on the body ,such as the left foot, right shoulder, and waist. The IMU's would be a part of a larger circuit that would involve a central microcontroller functioning both as a voltage distributor and as a processing hub for the raw data being recorded by the IMUs, as well as a battery for voltage supply. These two components would be placed on the waist, along with one of the IMU's.
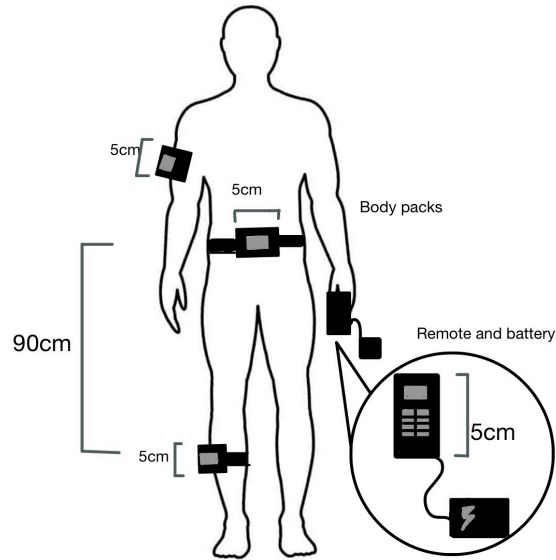
Figure 4: Accelerometers (IMUs) design diagram with dimensions. Remote and battery shown as well as individual unit locations [19].

Force Plate + Motion Capture

The design of the force plate and motion capture is centered around having force plate insoles in the skier's shoes. These force plates are portable devices that would be manually placed in the soles of the ski boots and would record reaction force and force distribution measurements. The motion capture aspect of the design would record 2-dimensional body images and segments of movement during the jump from multiple perspectives. This would include the angles of the body, the velocity of the jump, and the kinematics of the takeoff. The motion capture device would be a compact camera or mobile device suitable for outdoor usage, and would be placed directed towards the side view of the jump/jumper.
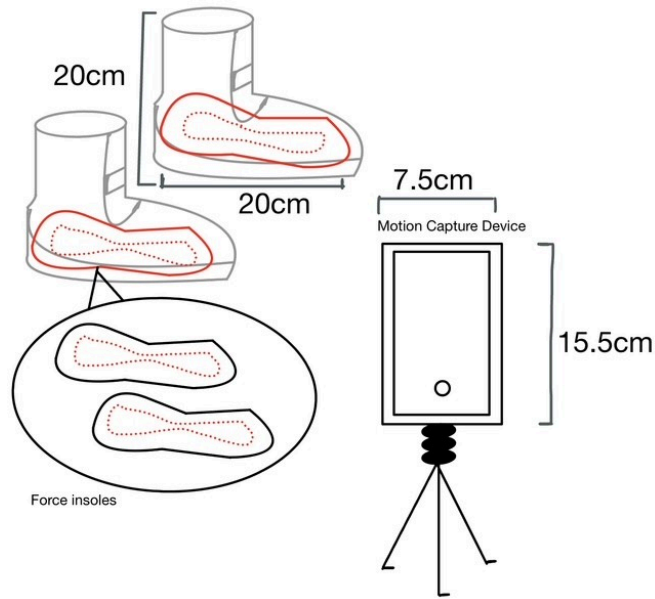
Figure 5: Force Plate + Motion Capture diagram with dimensions. Force insoles and motion capture device shown with tripod [20].

EMG Sensors

The EMG sensor system is aimed at capturing electrical signals of the ski jumper's muscles. The system includes a central hub that is wrapped around the user's waist or leg via a belt system and houses the microcontroller, filters, signal converters, and more. The electrodes are textile-based and are strategically placed around the athlete's body to capture signals from the most important muscles. The goal of this design is to provide insight into muscle activation patterns during the takeoff portion of the jump which may help athletes figure out optimal timing and coordination.
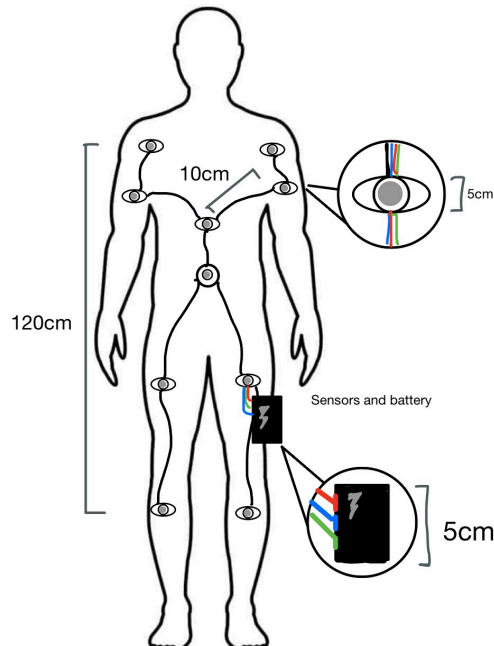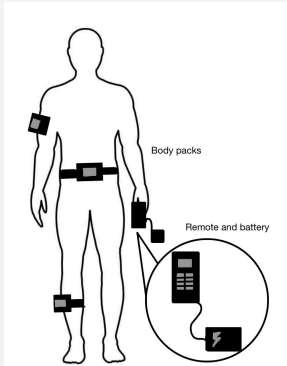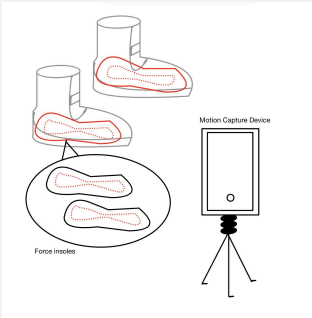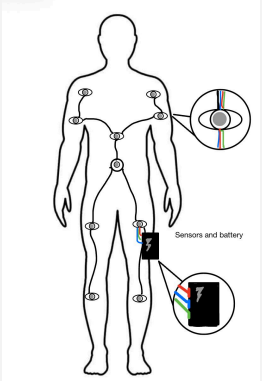
Figure 6: EMG Sensor diagram with dimensions. Suggested electrode placement and sensor/battery main unit shown [21].

Preliminary Design Evaluation

Design Matrix

The most critical design specifications were considered when creating the design matrix. Criteria are weighted and ordered based on importance. The winning design was the Force Plate Pressure Sensor combined with Motion Capture.

		Design 1: **Accelerometers (IMUS)** 		**Design 2:** **Force Plate + Motion Capture** 		**Design 3:** **EMG Sensors** 	
Criteria	Weight	Score	Weighted Score	Score	Weighted Score	Score	Weighted Score
Repeatability	25	3/5	15	5/5	25	2/5	10
Accuracy	25	3/5	15	4/5	20	4/5	20
Athlete Comfort/Interference	15	3/5	9	4/5	12	2/5	6
Ease of Use (Setup and Takedown)	10	4/5	8	4/5	8	2/5	4
Data Feasibility/ Processing Burden	10	1/5	2	4/5	8	3/5	6
Durability	5	4/5	4	4/5	4	2/5	2

Safety	5	5/5	5	5/5	5	5/5	5
Cost	5	5/5	5	3/5	3	5/5	5
Total (Out of 100):		63		85		58	

Table 1: Ski jump design matrix evaluating form of data collection.

Design Matrix Summary

The design matrix was used as an objective and quantitative method of determination of the best design for the specific form of data collection for the ski jump analysis system. The criteria chosen for this evaluation included: repeatability, accuracy, athlete comfort / interference, ease of use (setup and takedown), data feasibility / processing burden, durability, safety, and cost. Repeatability and accuracy were jointly ranked highest and were defined as the degree to which the same measurement system could produce the same results under the same conditions when repeated multiple times, and the proximity of a measured value to the actual, true, and accepted reference value, respectively. Because of the intensely dynamic nature of ski jumping, a system that could provide consistent, reliable results over the course of time was deemed paramount. The Force Plate + Motion Capture design was ranked highest in these categories because of its manual post-processing requirements and inherent lack of data disturbance caused by noise or circuit breakage. Because of the direct interaction between the system and the athletes themselves, athlete comfort/interference was deemed highly important. Again, the Force Plate + Motion Capture design was ranked highest because of the lack of system components that would need to be placed on the athlete directly. The lower-ranked designs contain more invasive component distributions and therefore have a higher chance of irritation, disturbance, and influence on athlete performance. Ease of Setup and Takedown and Data Feasibility were also considered. Defined as the ease to which the system can be setup and taken down each time the ski hill is visited, with relative consistency, and the practical possibility of data collection in the actual environment, outside of theoretical design, respectively, both categories again tended towards the Force Plate + Motion Sensor design because of inherent sensor characteristics of both the Accelerometers (IMUs) and EMG Sensors design. In an external environment, accelerometers utilize a global reference frame, which introduces a high probability of data error. EMG sensors require the consistent placement of electrodes on specific muscles across users, which introduces difficulty in the system setup. The last three categories, durability, safety, and cost, were important to consider, but did not provide much disparity between the designs. This lack of disparity in conjunction with their low weights, means they did not make significant impacts on the final conclusion of the matrix.

Proposed Final Design

The chosen design is the Force Plate + Motion Capture design. This design scored highest, or joint highest, in all categories besides cost. The Force Plate + Motion Capture design utilizes contemporary methods of ski jump analysis and applies quantitative analysis to allow for a comprehensive review of performance. The design is reliable, consistent, and minimizes athlete interference through use of noise-resistant and non-invasive methods. The system consists of force plate insoles made of velostat and PLA 3D printed insoles to track the generation of reaction forces and weight

distribution of the athlete. The data from the force plates is recorded on a microcontroller located in the back of the ski boot, which will translate the data onto a web application where the user can access the needed information to assess the jump. The motion capture part of this design is done with Kinovea, a 2-dimensional motion capture software to track vital angle development through the progression of the jump. Kinovea allows for the precise body angles of the skier to be measured and analyzed in a quantitative manner for performance assessment. The metric values derived from these components will be translated into concrete pieces of advice that will be given to the athlete, allowing for the direct improvement of jump score.

Fabrication

Circuitry

Materials:

The fabrication of the circuitry component of the product involved combining all hardware components necessary for the function of the device into one complex that can be housed together during product use. The complex components are as follows: an ESP32 Feather V2 microcontroller, which reads, processes, and wirelessly transmits sensor data to an online HTML user interface; an ISM330DHCX Inertial Measurement Unit, which measures foot orientation, acceleration, and motion; a 3.7 V Lithium-Ion battery, which provides portable power to the entire system; a slide switch that allows the user to manually turn the device on/off; and an LED indicator that tells the user when the device is on or off.

Methods:

The components were soldered together with wires and placed on a proto board for organizational purposes. The wire junctions were individually secured with either heat shrink or electrical tape. The lithium-ion battery, slider switch, and LED are a part of a sub-complex that can be manually removed from the microcontroller as the connection between the two is established through a JST connector, rather than soldered wire. This modular connection will allow the replacement of the entire sub-complex under the circumstance that the battery or LED stops working due to prolonged use or damage.
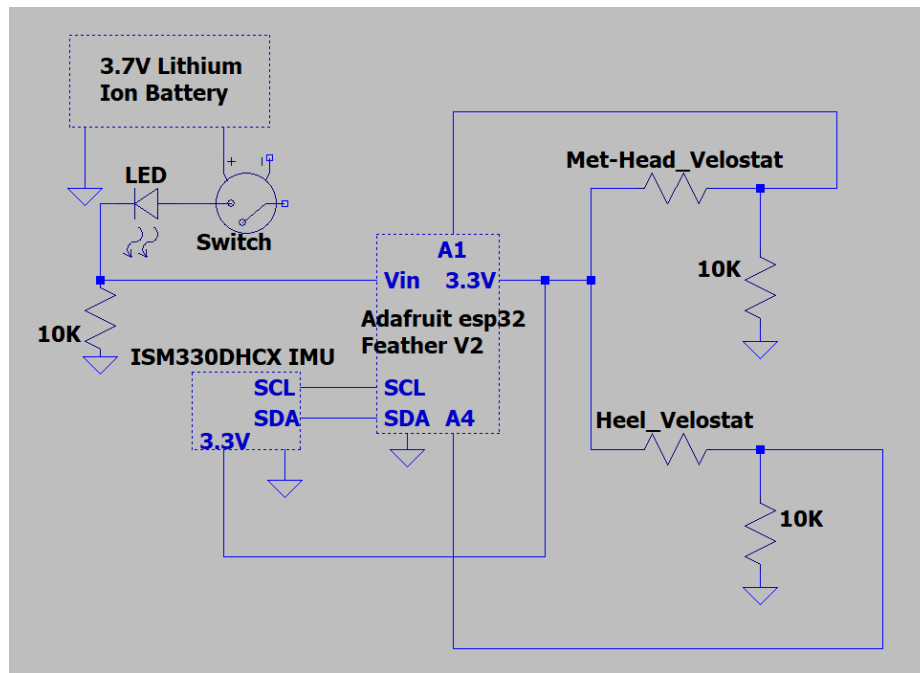
Final Prototype:

Figure 7: LTSpice Hardware diagram of the entire electronic circuit of the Force Insole system, including all components within the housing unit.

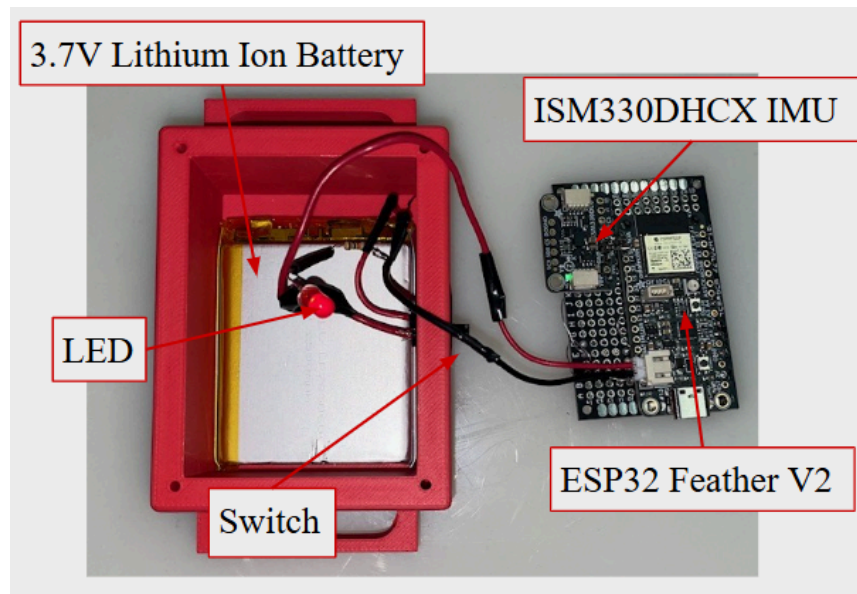*Figure 8: Full microcontroller circuit with individual component labels and housing unit.*

Housing Unit

Materials:

The fabrication of the microcontroller housing unit included 3D-printing both the housing unit and the lid in PLA. PLA was the selected material as it is sturdy and non-corrosive, which is necessary for the conditions in which ski jumping is practiced. Specifically, the conditions associated with winters in the midwest as defined by the Wisconsin Climatology Office (see Appendix A: Preliminary Design Specification). If a less durable material had been chosen, the harsh weather conditions associated with Wisconsin winter could degrade the housing unit and the microcontroller inside, rendering all data collected either lost or negatively impacted in some way from the freezing cold and harsh wind conditions.
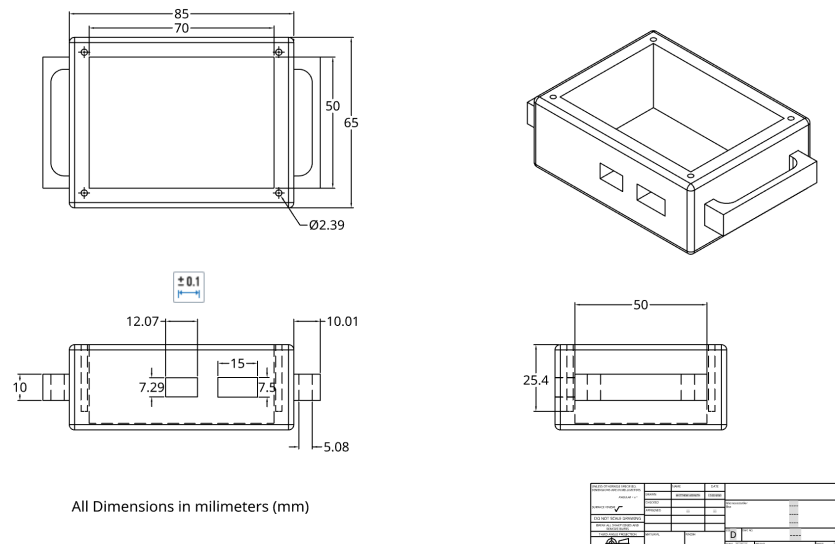
Figure 9: Microcontroller housing unit isometric and orthographic views of the finalized microcontroller enclosure, showing mounting hole locations, side-wall cutouts, and overall dimensions (mm) used for fabrication and component integration.

Methods:

To create the microcontroller housing unit, a CAD model in OnShape was created using planned dimensions to fit the microcontroller complex and allow wires to connect from the microcontroller in the box to the force insoles outside the box. While planning the dimensions, the housing unit was scaled down more than enough to fit within the compact size parameters defined to relevant DHS standards (see Appendix A: Preliminary Design Specification). Once the CAD model was completed, it was then 3D printed in PLA twice for the pair of force plate insoles. Post-print modifications were then implemented to bring the units to their final design. Four brass inserts were melted 1 cm deep in each corner to screw the lid into, and an LED hole was drilled adjacent to the switch and wire openings on the front face. Each individual opening was sanded and deburred to remove any rough surface finish. Further breakdown of fabrication methodology can be observed in the appendix. (see Appendix D: Housing Unit Fabrication Protocol).

Final Prototype:
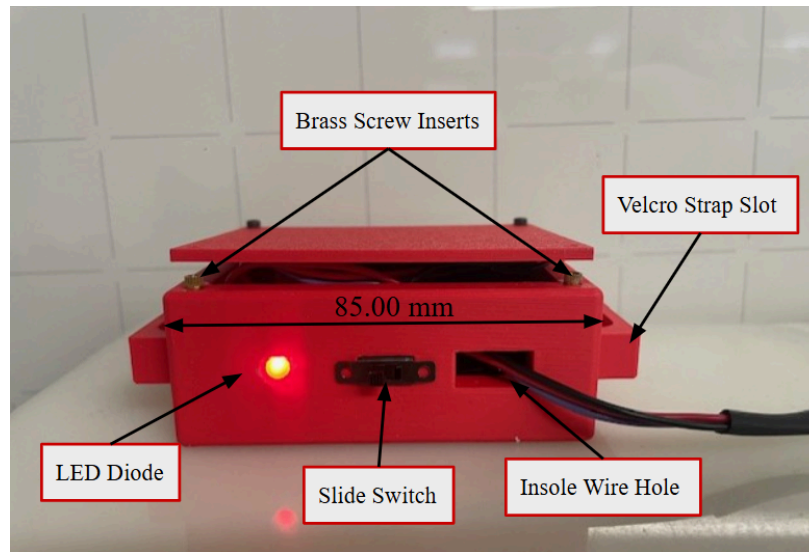
Figure 10: Microcontroller housing unit with full circuit plugged in and activated.

3D Printed Force Insoles

Materials:

The custom fabrication of the force insoles include individually sized 3D-Printed PLA templates, Velostat which is a piezoresistive composite polymer whose resistance changes due to flexion for compression [22], electrical tape to insulate everything except the Velostat regions and anchor the components, copper tape as a conductive trace between the sensors and the controller, 10 kΩ resistors that create voltage divider circuits for reading the Velostat's variable resistance, and thin gauge wire connecting the copper tape to the entire circuit complex aforementioned.
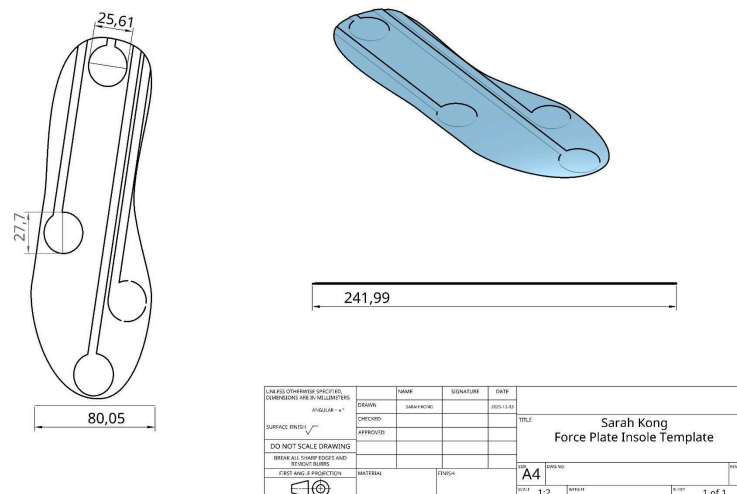
Figure 11: Insole Isometric and orthographic views of the finalized insole template, showing specific Velostat and copper tape traces, and overall dimensions (mm) used for fabrication and component integration.

Methods:

To construct the force insoles, a template is first 3D-printed according to the size of the user's ski boot size [23]. Velostat, an electrically conductive material whose resistance changes due to flexion or compression, is then placed to the bottom of the template at the ball and heel, which is then secured with electrical tape. Connected to the Velostat is copper tape leading to the back end of the insole, where it is soldered to the electrical wiring leading out of the boot and into the housing unit, attached to the microcontroller. For a Velostat sensor to work, it must be insulated and sandwiched between two conductive layers (copper tape in this case), as it is a carbon-impregnated plastic, meaning its electrical resistance changes predictably in response to physical pressure. The copper serves as the two contact points needed to complete the circuit and measure the material's variable resistance. The original insole design featured four Velostat sensors, positioned on the heel, first metatarsal head, tip of the second metatarsal, and just below the fifth metatarsal head, as indicated on the software template. This arrangement would have allowed a more detailed analysis of foot placement and weight distribution, but it increased circuit complexity and the risk of damage. Significant pronation and supination of the foot do not occur during a ski jump due to its largely linear trajectory and the stiff nature of ski boots, eliminating the need to differentiate between the left and right sides of the foot [24]. Consequently, the design was simplified to two larger Velostat sensors, covering the heel and the ball of the foot. This configuration provides insight into weight distribution between the front and back of the foot, as well as overall ground reaction forces, while reducing complexity and potential failure points.

Final Prototype:

Figure 12: Force Insole copper tape wiring and Velostat placement diagram.

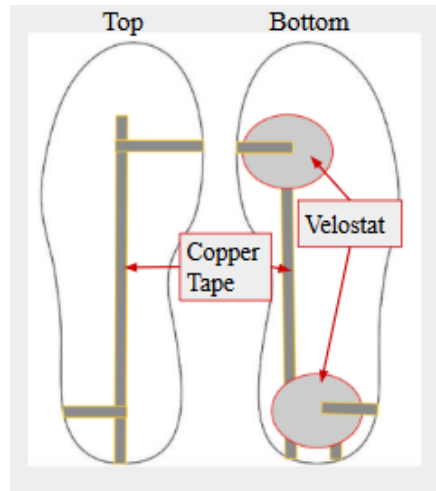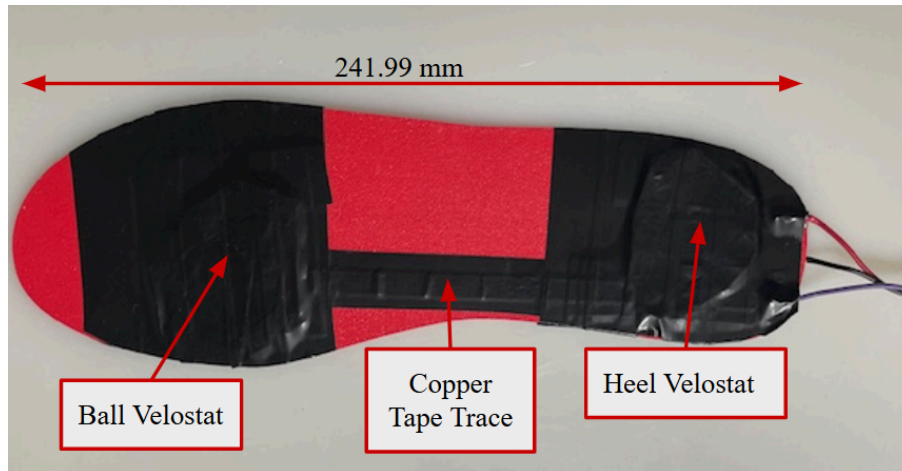*Figure 13: Force Insole Final Prototype with electric tape covering velostat sensor and copper tape traces with microcontroller wiring protruding from heel.*

Final Training System

The final design is a cohesive data collection system composed of force insoles, an inertial measurement unit, and motion capture done through Kinovea, which together, track numerous specific data metrics of any given ski jump. The design utilizes contemporary methods of ski jump analysis and applies quantitative methods of jump characterization and feedback to allow for a comprehensive review of performance. The circuit is built around a central microcontroller that serves as the hub for data collection, storage, and processing from both the inertial measurement unit and the force plates. Power is provided by a lithium-ion battery, which can be manually controlled via a slider switch. The complete system is securely housed within a custom 3D-printed PLA enclosure, ensuring durability and portability. The final housing unit design has specific rectangular dimensions (8.5 cm x 6.5 cm x 3.25 cm) to snugly fit the battery and microcontroller complex, whilst still having ample room for the switch, LED, and insole wires to comfortably align with the three holes on the front face. The housing unit is attached to the back of the boot via a velcro strap to avoid extra drag force that would be created by the increased lateral surface area induced by the unit. The force plate insoles in the system are made of Velostat and PLA 3D-printed insoles to track the generation of reaction forces and weight distribution of the athlete. There are two distinct Velostat locations, one on the ball, and one on the heel of the foot. These locations provide, in singularity, an evaluation of ground reaction force put into the jump by the athlete, and together, a simple comparison of force distribution in the foot indicating forward or backward tending body weight displacement. The inertial measurement unit, IMU, is a 6-axis accelerometer and gyroscope that is used to track three-dimensional linear velocity of the ski jumper. The signals from both the Velostat and the inertial measurement unit are recorded by the microcontroller, which translates the data and uploads it onto an online HTML interface where the user can observe and download the quantitative information necessary to assess the jump. The motion capture part of this design is done with Kinovea, a 2-dimensional open-source biomechanical motion capture software, that is used to track specifically the knee and ankle angle development of the athlete through the progression of the jump. Used in tandem, the metric values derived through the various data tracking apparati within the system provide a quantitative basis of characterization for a single jump, which will help build the objective evaluation of athlete performance desired.

Figure 14: Final circuit design with the housing unit attached to a ski jumping boot via a velcro strap.

Software

      The software logic flow of the system can be observed in Figure 15. It visually describes the basic path of data as it is first sensed, processed and finally received on the user's end via the HTML online interface. The ESP32 microcontroller acts as the fulcrum of data processing and output, allowing the stimuli being received at various sensors in the system to be turned into pieces of logical data that have actual meaning and implication.
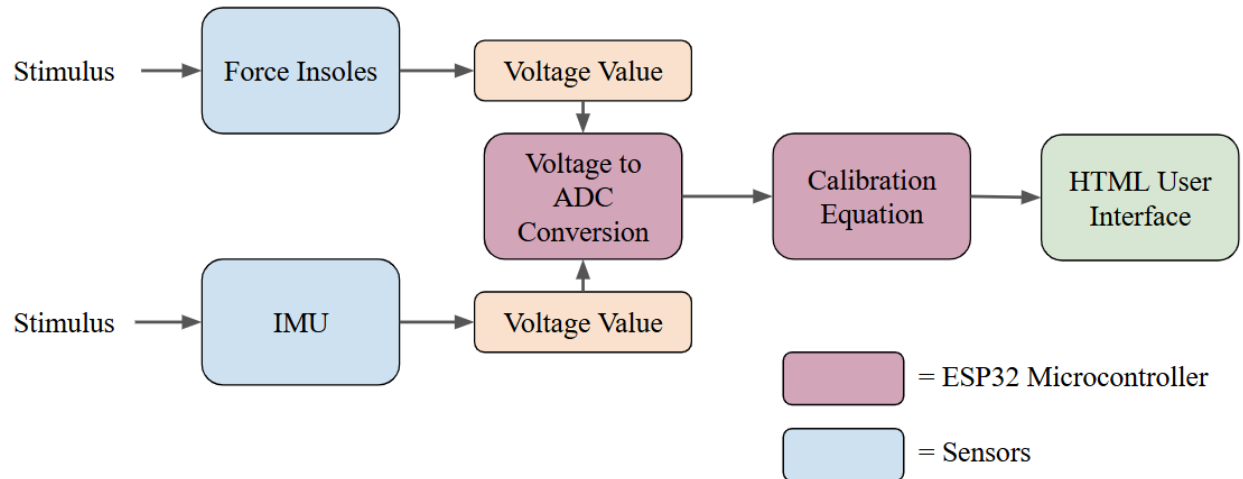
Figure 15: Final Prototype Software Flow Diagram of data stimulus to user-end acquisition.

The sensors first convert the received stimuli into voltage signals via their hardware circuitry. These voltages are then processed and translated into meaningful measurements using experimentally determined calibration curves. The resulting values are displayed to the user through the online interface, as shown in Figure 16.
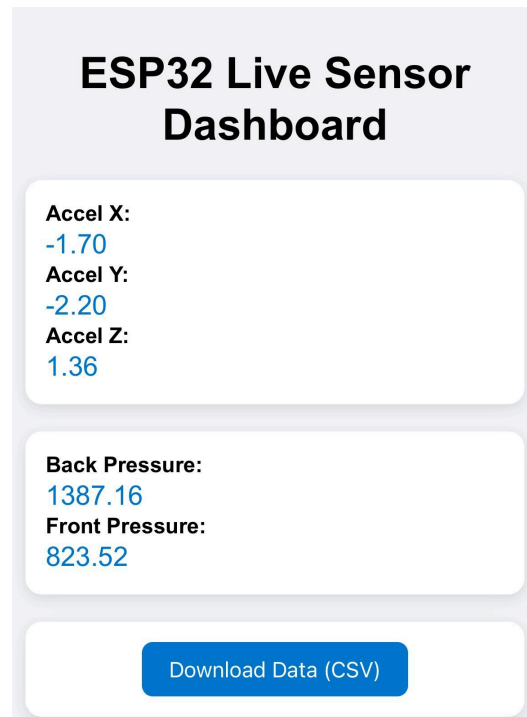
Figure 16: ESP32 HTML Online User Interface Sensor Dashboard

The mathematical description of the circuit and the ESP32's internal processing is found below, where the formulas utilized are derived from internal characteristics of the microcontroller, the hardware configuration, and performed calibration tests. The Velostat, as previously described, acts as a resistive

element within the circuit. It provides a corresponding resistance value through a pressure stimulus which can be directly identified when placed within a voltage divider circuit. This voltage value is then stored as an appropriate correlating integer value within the ESP32 memory known as an ADC value. This value can then be reverse calculated into a voltage value, further into a resistance value, or converted into a separate metric, such as force, through an identified quantitative relationship, as done in this case.

Circuit and ESP32 Internal Calculations

Ohms Law states that a voltage supplied across a resistor is directly proportional to the current running across that same resistor [25]. Kirchhoff's Voltage Law states that the sum of all voltage within a closed system is equal to zero, or more simply the sum of voltage drops across the resistors in a closed circuit are equal to the voltage supplied [26]. Using both laws in tandem allows for the derivation of an equation involving the Velostat's resistance giving an output value, V_{out}. The final V_{out} value obtained from this manipulation is what links the force insoles to the microcontroller. It indicates how much voltage the microcontroller will be receiving from a given stimulus based on the corresponding resistance value of the Velostat material. When the V_{out} reaches the ESP32, it is internally processed through an integer-based analog to digital conversion storage system. The microcontroller requires this conversion to understand what the value is, what it means, and what it needs to do with the value. The specific ADC value is the binary product of the microcontroller quantizing the voltage stimulus into the bit capacity of its storage memory to link a received voltage value to a readable placeholder [27]. Once in the microcontroller's storage memory, a derived force calibration curve will indicate which Velostat resistance value correlates to what quantity of force applied on the Velostat sensor. These values when used in singularity or in comparison to others will directly tell jump force and foot positioning respectively, which can be used as metrics for ski jump improvement.

Velostat Voltage Divider:

Beginning with Ohm's Law, the equation can be rewritten in terms of the current, I;

$$V = IR \rightarrow V/R = I \quad ; \quad (Ohms\ Law)$$

Understanding that the current will be constant in a closed loop, it can be rewritten as;

$$V/R = V/R$$

And further in terms of the system;

$$(V_{out} - V_{in}) / R_{velostat} = (\text{Gnd} - V_{in}) / (R_{velostat} + R_{constant})$$

Seeing as Gnd = 0 V, it can be rewritten in terms of V_{out};

$$V_{out} = V_{in} * (R_{constant} / (R_{velostat} + R_{constant})) \quad ; \quad (\text{Basic } Voltage\ Divider\ Equation)$$

Plugging in system specific values;

$$V_{in} = 3.30\ V$$

$$R_{constant} = 10\ k\Omega$$

$$\mathbf{V_{out} = 3.30 * (10{,}000 / (R_{velostat} + 10{,}000))}$$

This is the equation the microcontroller uses to apply quantitative meaning from a force insole pressure stimulus.

ESP32 ADC Value:

$$\text{ESP32 Feather V2} \rightarrow 12 \text{ bit on base power 2 scale} \rightarrow 2^{12} = 4096$$

The microcontroller has 4,096 individual integer values to characterize a received voltage stimulus, anywhere from 0 - 3.30 V.

$$V_{out} * 4096 / 3.30 = \text{internal assigned ADC value}$$

Calibrated Force Equation:

$$x = \text{Ground Reaction Force}$$

$$y = \text{ADC Value}$$

$$y = 662.58\, e^{0.0006x}$$
$$x = ln\,(y / 662.58) / 0.0006$$

Testing and Results

Force Plate Calibration Curve

As mentioned in the software explanation, the circuitry, including the force plate and microcontroller, outputs a discrete data value called an ADCvalue. This ADC value has no inherent meaning in terms of its value for coaches to provide quantitative feedback to their athletes, as outlined in the PDS. To fix this, there needs to be a calibration curve that relates the ADC value to a vertical ground reaction force (vGRF) metric in Newtons (N). This commonly used force value is the standard for any force plate system and represents the upward force that the ground exerts on the body when it is in contact with a surface. According to Newton's third law, when a ski jumper pushes into the ramp/ground with a certain force, an equal and opposite force is pushed back by the ramp/ground [28]. Through discussion with the Blackhawk Ski Club Ski Jumping coach, one major issue with youth ski jumpers is their refusal to jump with full exertion as they came down the ramp. Often, they applied only a little force to their jump, which results in the athlete sliding out of the ramp instead of jumping off it, thereby affecting their form and distance. With force insoles that can output this vGRF value in a curve over time, coaches can provide immediate feedback to their athletes, encouraging them to jump harder and apply more force to the ground. Athletes who were apprehensive about jumping can now utilize this biofeedback to help their bodies overcome their previous fear or confusion about how to jump.

The first idea to relate ADC to vGRF was to use weights ranging from five to twenty pounds in the teaching lab. This would give a known vGRF value by converting pounds to kilograms. Then, the use of the F = mg calculation, where m is the weight in kilograms and g is the acceleration of gravity, can provide an output force [29]. However, through preliminary testing on our force insole prototype, it was discovered that the velostat did not respond well to constant forces. When a weight was placed on the insole, the ADC would jump initially, but instead of staying constant at the new value, it would begin to

drop back down. Another issue with this method was the need to extrapolate the force curve from real-world jumping. The weights procedure was correlating the ADC with low vGRF values, not the 3x body weight forces that the insoles would need to withstand per the PDS. More realistic forces were needed to generate the curve.

The method that was ultimately chosen was placing the force insoles on the top of the teaching lab's professional Bertec Acquire Force Plates. The force plates were initially turned on and zeroed. Fz was isolated, as this correlates with vGRF. Then the tester placed our force insoles on top of the plate and brought a chair to the edge of the plate. During a preliminary meeting, the ski coach mentioned that they would train with chairs to simulate the in-run position. The tester assumed the ski jump position before takeoff by sitting on the edge of the chair and bending forward at the hips. The tester then placed one foot on the ski jump insole, which was over the velostat sensors and on the force plate. The tester exited the ski jump position and jumped off the insole and plate. During this test run, the Bertec Force Plate software was used to record and capture the vGRF data in a CSV file. After finishing the run, the force insoles were unplugged to pause the ADC data collection in the microcontroller. Both ADC and vGRF data were opened, and the peaks were matched and recorded on a data table found in Appendix F. Since the force insole ADC value did not start at zero, the change in the ADC value was found by locating the consistent ADC "zero" value before the tester jumped and recorded it for analysis. In the end, there were 21 simulated jump data points, and they were split into thirds based on low, medium, and high exertion levels.

After recording the ADC values from the force insoles and the vGRF values from the force plates, the data were transferred into an Excel spreadsheet. The plot tool was used to create a scatter graph and assigned an exponential trendline: $y = 662.58e^{\wedge}0.0006x$. The R^2 correlation coefficient was 0.523, indicating a moderate correlation. Velostat's non-linear force and voltage responses cause small force changes for low loads. Large loads bring about significant changes due to material flattening and saturation of the internal conductive path. The exponential trendline accurately represents the curve's behavior. The moderate R^2 value reflects velostat as a sensor material. Velostat is known for variability and sensitivity to foot placement, which affects its ability to output perfect correlation to applied loads.

Finally, a trendline equation was added to the force insole microcontroller code to output ADC correlated force values via our Wi-Fi interface.
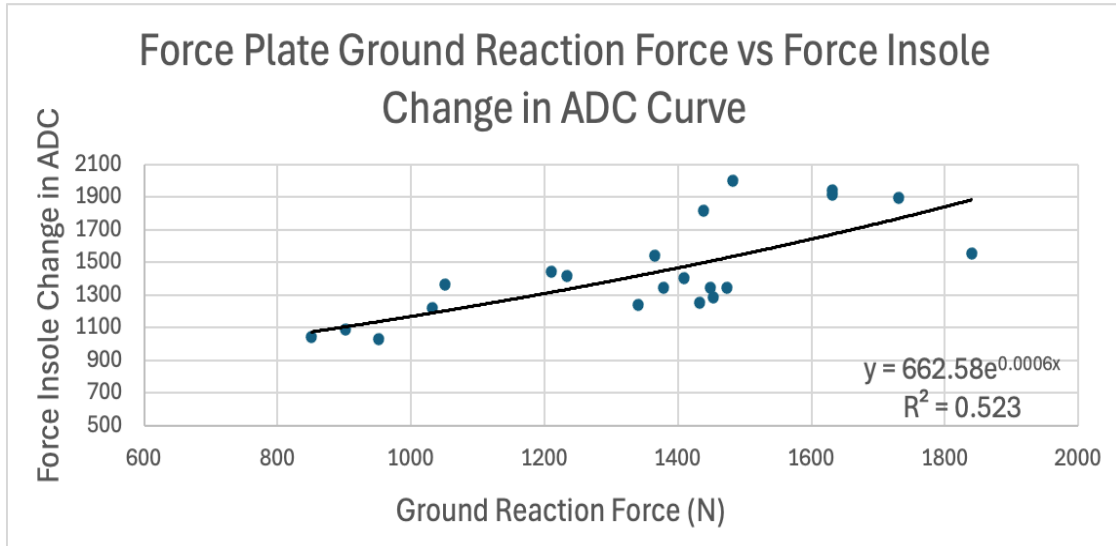
Figure 17: Force Plate Insole Calibration curve with exponential trendline $y = 662.58e^{\wedge}0.0006x$ and R^2 = 0.523 relating discrete ADC value to output vGRF.

Force Plate Testing and Curve

        The generation and analysis of multiple force graphs to ensure the functionality of the force insole system in its entirety, including both the collection and processing of force data, a qualitative assessment of the generation and analysis of multiple force graphs, analogous to the one in Figure 18, was performed. This testing procedure can be described as a qualitative assessment that ensures the force insoles are parsing vGRF input and outputting the correct output curve. Once most of the final prototype was developed, the finished insoles were placed on the ground and stepped on three times while putting force into the ground through partial jumps. While this was happening the Wifi interface opened to record the collected data and then saved the CSV file with the vGRF data for both the forefoot and heel sensors. The CSV files were then inserted into MATLAB and graphed the two sensor vGRF curves while highlighting peak values, removed baseline noise, and converted the time values to seconds.
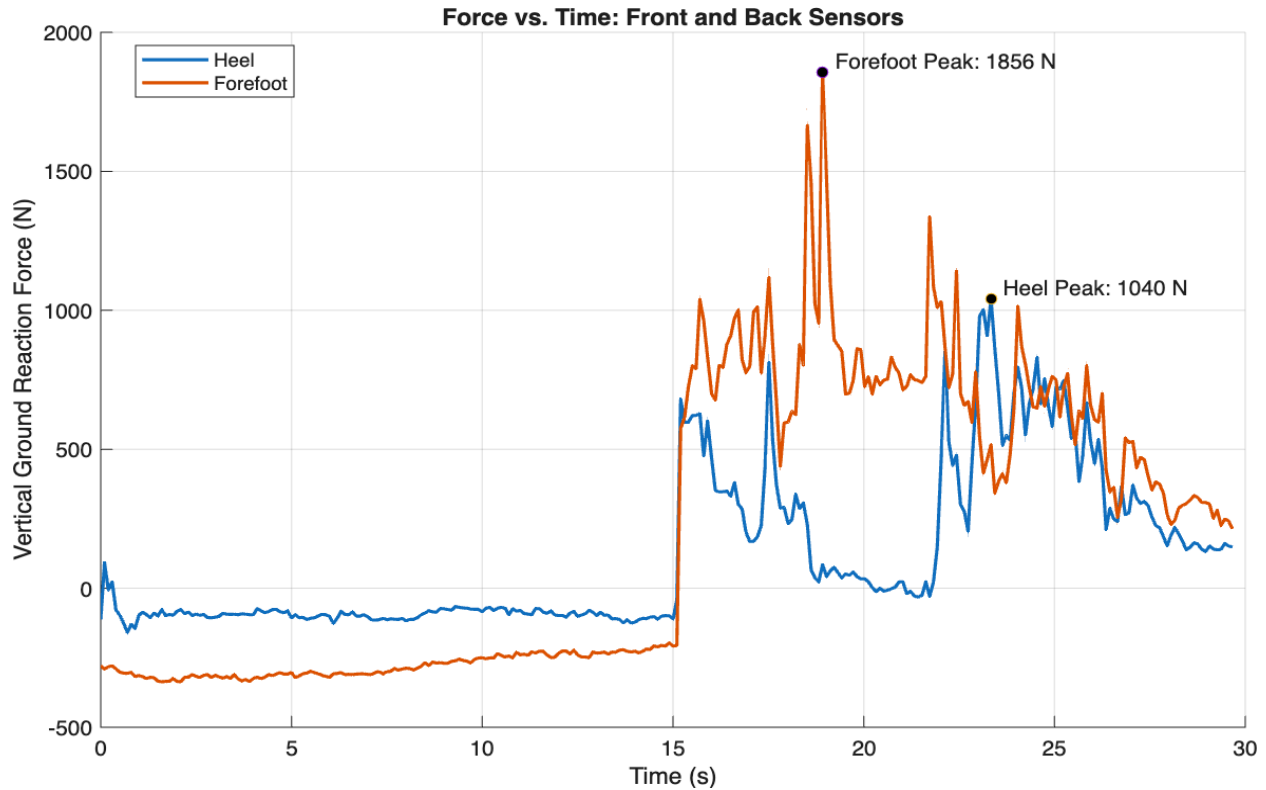
Figure 18: vGRF curve with respect to time for forefoot and heel velostat sensors in force plate insoles for three trial jumps.

Kinovea 2D Motion Analysis

To begin to build a foundation of data for the future designation of correlational relationships between jump performance and quantitative angle metrics of the athletes, as well as to demonstrate the functionality of the Kinovea 2D motion video analysis software, numerous slow-motion videos of individual youth ski athletes at Blackhawk Ski Club were analyzed for the progression of both knee and ankle angles. These knee and ankle angles can be more accurately described by observing Figure 3, which designates θ Knee and θ Ankle, respectively. The knee angle chosen for this analysis was the joint internal knee angle, or the angle between the thigh and the shank that represents knee flexion. The ankle angle was the angle between the skis and the athlete's shin, commonly referred to as the shin angle.

For this process, multiple Blackhawk Ski Club practices were attended to ensure proper video quality and adequate data collection. The initial visit included the entire group and was useful for gaining a sense of the scope of the ski hill, as well as potential spots that would allow for recording the takeoff ramp at a perpendicular angle and distance, thereby preventing video angle distortions due to non-perpendicular shot angles. The coach also mentioned clearing out some of the trees next to the forest line so that recording could occur farther away from the ramp, thereby minimizing lens distortion effects from the camera. The second time at the hill was a test recording visit during one of the afternoon practice sessions, where an iPhone slow-motion video was recorded at a 60 Hz frequency and 1080p resolution. This session ended with videos to test and determine the angle recording protocol in Kinovea; however,

26

the footage was too dark and grainy to yield accurate estimations of the marker positions. The glare from the light on the hill also affected the video quality, and the number of skiers recorded was limited to two local athletes. The third visit was a recording day during a joint ski jumping training session with athletes from across the Midwest. This time, the recording device was a Sony RX100 VII camera that was capable of 1080p at 120 fps, providing improved video quality and smoother slow motion too. This event was also held during the day, which resolved the glare issue present in the nighttime shots. Finally, ski jumping data was obtained for more than six athletes and settled on ski jumpers 1 (USA outfit) and 2 (Green/Black outfit) for our final analysis, due to the quality of their jumps compared to those of the other athletes. After loading the slow-motion footage and setting up tracking markers for each individual on Kinoeva, the auto marker tracker was used to collect data for four jumps from each angle. Many manual adjustments were required to the marker positions, as the software would lose positioning, causing the angles to change and the markers to drift off. Once these were completed, the angle data CSV was loaded into MATLAB, and displays of the knee and ankle angles were created with respect to the time of the jump for the two athletes. This plot focuses solely on the angle changes during the end of the in-run, leading into the takeoff, and some of the early flight, or the portion of the jump most critical for scoring.
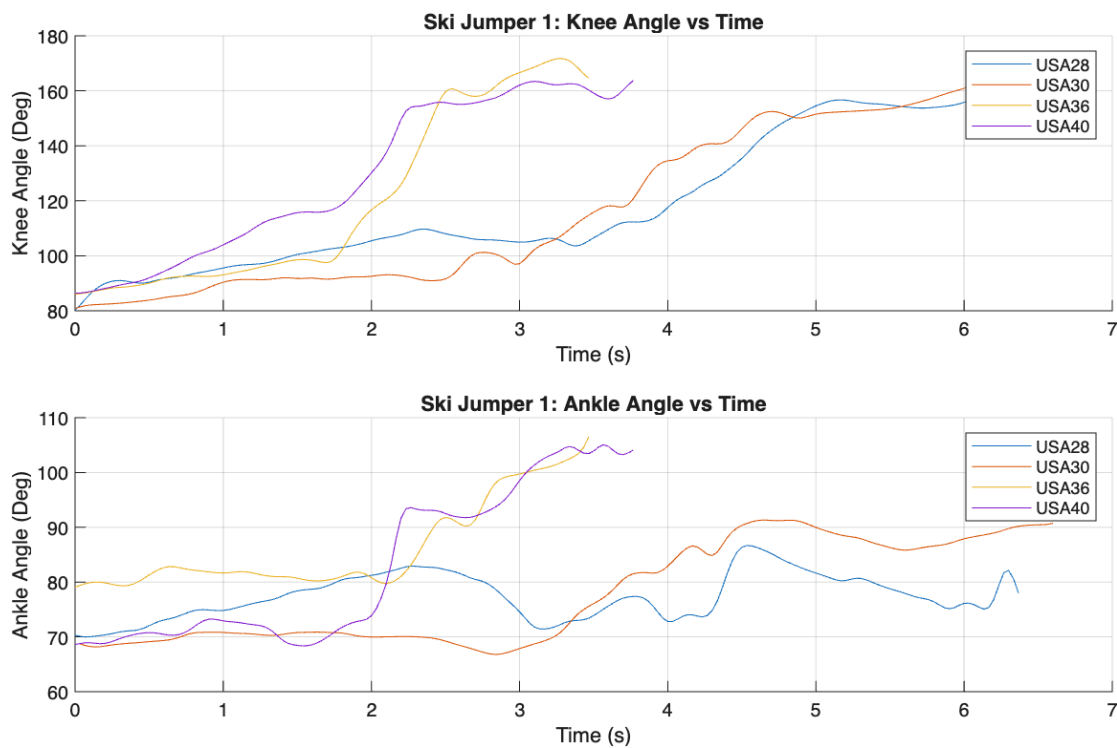
Figure 19: Ankle and Knee angle with respect to time for four jumps performed by Ski Jumper 1 (USA outfit).
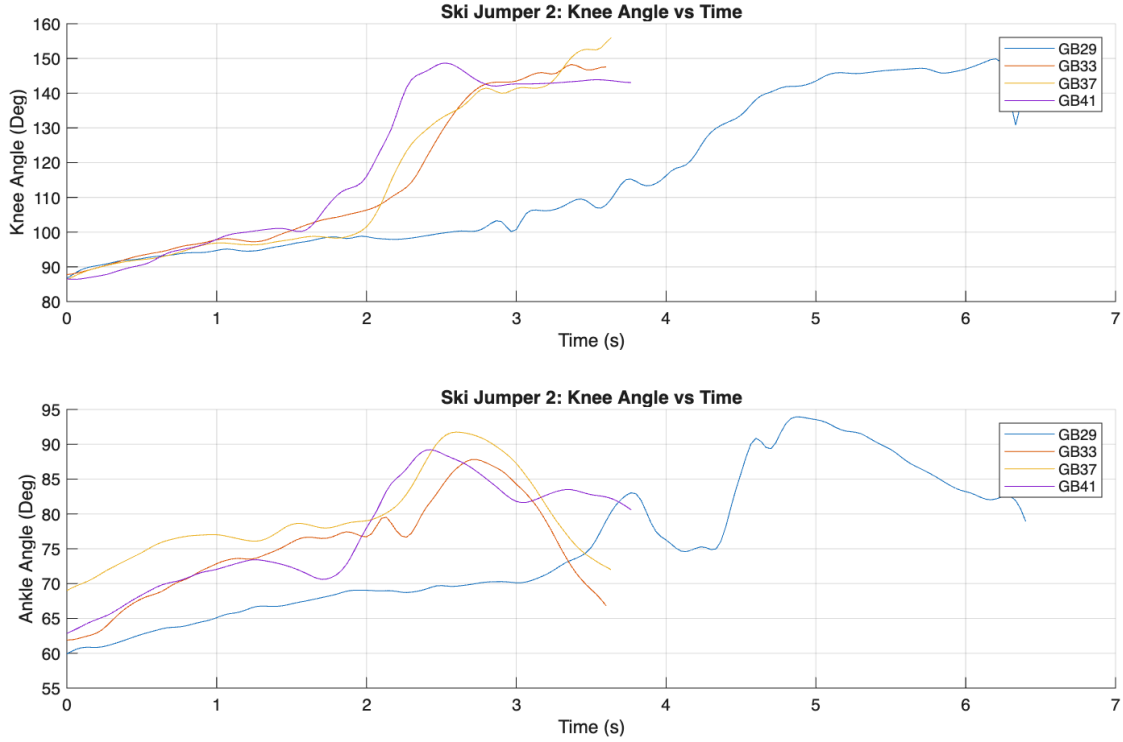
Figure 20: Ankle and Knee angle with respect to time for four jumps performed by Ski Jumper 2 (Green/Black outfit).

Discussion

Physics/Graph Analysis

The knee and ankle angle graphs collected during the jumper's in-run and takeoff provide the coach with clear, quantitative information to guide athlete feedback. Across the trials, jumps with a more gradual increase in joint angles, particularly USA28 and USA30, demonstrate a smoother extension pattern during the takeoff. A gradual slope is more desirable because it indicates that the athlete is maintaining the aerodynamic in-run posture longer and transitioning into the takeoff without prematurely bringing their torso up and increasing drag. Prior research emphasizes this concept of a controlled lower-body joint extension to generate impulse while preserving low drag until the final moment of takeoff. To further interpret these kinematic patterns, this classical model of ski-jumping in-run velocity helps describe how gravity, drag, and friction interact to determine a jumper's speed:

$v = \pm\sqrt{\frac{g(sin(\theta) - \mu cos(\theta))}{cA\frac{\rho}{2m}}(1 - e^{-2cA\frac{\rho}{2m}s})}$ [28]. This model shows that the jumper achieves maximal

in-run velocity if the mass (m) is increased and if the coefficient of friction (μ), air density (ρ), surface area perpendicular to the direction of motion (A), and the drag coefficient (c) are all decreased. The model and the recorded kinematic patterns that the team gathered support the conclusion that controlled, sustained aerodynamic posture leads to higher velocity and further jump distance. When comparing the start of the angle curves between jumper 1 and 2, there is more consistent in-run body positioning for

jumper 1. This means they are tucked in for all their jumps, resulting in lower surface area and reduced drag, increasing their speed before takeoff.

Additionally, the vertical ground-reaction force (vGRF) profiles recorded from the heel and forefoot sensors provide insight into whether youth jumpers are actively pushing off the hill or merely sliding off. That data shows a forefoot-dominant force peak of 1856 N and a secondary heel peak of 1040 N, which is consistent with the forward shift of the center of pressure expected during the takeoff motion. These results are in concurrence with other research studies that correlate a further jump distance with a sharp vGRF peak at the forefront of the foot, specifically at the big toe, at the moment of the jump [29].

Ethical Considerations

Because this project involved human subjects, several ethical considerations guided both the data-collection process and the intended use of the device. All participants and their legal guardians provided informed consent and assent, and the athletes and coaches were made aware of the study goals and procedures before participation. Athlete comfort was taken into consideration throughout the entirety of the project to ensure the force insoles and motion capture system did not alter the youth athlete's natural jumping technique, introduce safety risks, or place additional physical demands on the athletes. Data privacy is also a priority; all kinematic and force data are stored securely and used solely for research and training-support purposes. On top of these human subject considerations, it is also important to address the ethical implications of implementing biomechanical monitoring devices in a youth sports environment. Technology-enabled feedback can be beneficial, but it must be used in a way that supports athlete development rather than creating performance pressure or inequity within the Blackhawk Ski Jumping team. The device is framed as a teaching and learning tool, not a metric for ranking athletes or a necessity for athletic advancement.

Project Complications

Since the project was designed for our client at Blackhawk Ski Club, it was intended to be tested on ski jumpers there during their season. However, the ski club closed at an earlier date due to winter preparations on short notice. This caused a major limitation to the amount of data that could be collected, which was a potential source of error. These potential errors include a lack of varied data, few opportunities to compare insole data with jump quality, and more reliance on repeatable lab testing. This altered the path of the testing process, and the force insoles have not yet been tested on youth ski jumpers. Instead, the insoles were tested at the University of Wisconsin - Madison's teaching lab. The potential errors of not being able to compare insole data to real take-offs were avoided by mimicking the in-run mechanics of the body during the jump while stepping onto the plate. This allowed for the force plates to be calibrated and validated for data collection. Thus, these situations allowed for the project to be altered to a higher reliability and repeatability.

Sources of Error and Future Changes

A source of error in the force plate insole is the design choice of Velostat as the sensor. Although Velostat is a very thin material and allows for a very non-invasive force plate insole design, it struggles to stay consistent in accurately outputting the forces as accurately. This is why our correlation curve had

only a moderate R^2 value, which is not ideal for accurate force collection but enough to see differences in vGRF between jumps. One change in the future of this design could be looking into strain gauge cells that are thin enough to be embedded into a softer insole. This way, the force output will be based on physical changes within the sensors via strain rather than changes in resistance due to Velostat stretching.

Another source of error comes from the 2D motion capture video analysis, where the auto marker tracking feature was used to track angles throughout the jump. This auto marker tracking feature uses a pixel color algorithm to stay in the same spot of the ski jumper as the video plays, but since there were so many color differences in the outside video, the marker would be occluded and dragged off. This required lots of manual work to get the marker back to the right part of the ski jumper's body to keep the angle consistent. This means our angles tracked over time weren't fully accurate due to human error, though manual adjustments were made. Next time there is a collection of video data for the ski jumpers, it would be beneficial to put bright white markers or stickers on their hip, knee, and ankle areas, or wherever an angle has to be calculated, so that the auto-tracking feature works more accurately.

Conclusions

The project is a biomechanical research study on ski jumping that utilizes a data collection system allowing youth ski jumpers to receive data-driven feedback and improve their technical skills. The data collection system integrates motion capture and force-sensing insoles to collect body angles and ground reaction forces during the in-run, takeoff, and early flight phases of the jump. The system will then provide coaches with targeted, evidence-based feedback that can guide ski jumper training to optimize performance and bridge the gap between amateur and professional performance. The development of the system introduces a new quantitative approach to coaching feedback in ski jumping, opposing the traditional method of subjective perception of each jump.

This project has the potential to significantly improve how ski jumping technique is taught and evaluated. With the implementation of wearable force insoles and motion-capture analysis, coaches can now quantify elements of performance that are normally judged visually. This provides a platform for athletes to receive clearer and more actionable feedback supporting a more consistent development of skills. More broadly, this technology moves ski jumping toward a more modern, data-driven training model similar to advancements seen in other sports. By generating reliable force and kinematic profiles, the device can help establish standardized benchmarks, improve coaching equity, and create long-term performance databases that benefit athletes and programs at all levels. Ultimately, this design contributes to a shift from qualitative judgment to evidence-based coaching, offering a meaningful opportunity to elevate both performance and safety in the sport.

Future Work

The continuation of the project would focus on applying the newly developed analysis tools to begin to build quantitative relationships of measured performance metrics and jump outcome, relationships that are currently absent from formal ski jump training. This process would involve using the force plates and Kionvea in tandem, on ski jumpers at the Blackhawk Ski Club, to collect a large pool of data. Each jump's specific metric value would be linked to the judged jump performance by professional judges and coaches, and from there, optimal and suboptimal values can be determined. Once these correlational relationships are established, the user interface would be modified for a more feedback based approach

which would allow coaches to easily take athlete-specific data and curate personalized feedback to improve athlete performance.

References

[1] "The history of ski jumping: from the beginning to today." Accessed: Oct. 08, 2025. [Online]. Available: https://www.redbull.com/au-en/ski-jumping-history

[2] "Leveraging Video Analysis in Sports: Techniques, Tools, and Coaching Insights – Sports Analytics and Performance Modeling." Accessed: Oct. 08, 2025. [Online]. Available: https://harvardsciencereview.org/2025/07/09/leveraging-video-analysis-in-sports-techniques-tools-and-coaching-insights/

[3] "AI Sports Video Analysis 2025: Revolutionary Performance Insights The Fitness Engineer." Accessed: Oct. 08, 2025. [Online]. Available: https://ai-fitness-engineer.com/ai-sports-video-analysis

[4] O. Elfmark *et al.*, "Performance Analysis in Ski Jumping with a Differential Global Navigation Satellite System and Video-Based Pose Estimation," *Sensors*, vol. 21, no. 16, p. 5318, Jan. 2021, doi: 10.3390/s21165318.

[5] D. Stepec and D. Skocaj, "Video-Based Ski Jump Style Scoring from Pose Trajectory," in *2022 IEEE/CVF Winter Conference on Applications of Computer Vision Workshops (WACVW)*, Waikoloa, HI, USA: IEEE, Jan. 2022, pp. 682–690. doi: 10.1109/WACVW54805.2022.00075.

[6] "Sensor insoles for clinical grade mobile gait & motion analysis." Accessed: Oct. 08, 2025. [Online]. Available: https://moticon.com/

[7] J. Yu *et al.*, "Key transition technology of ski jumping based on inertial motion unit, kinematics and dynamics," *Biomed. Eng. OnLine*, vol. 22, no. 1, p. 21, Mar. 2023, doi: 10.1186/s12938-023-01087-x.

[8] "Biomechanics in ski jumping: A review - Schwameder - 2001 - European Journal of Sport Science - Wiley Online Library." Accessed: Oct. 08, 2025. [Online]. Available: https://onlinelibrary.wiley.com/doi/10.1080/17461390100071107

[9] "Performance and Biomechanics in the Flight Period of Ski Jumping: Influence of Ski Attitude." Accessed: Oct. 08, 2025. [Online]. Available: https://www.mdpi.com/2079-7737/11/5/671

[10] W. Liu, F. Lu, X. Suo, and W. Tang, "Optimization of ski jumping in-run posture using computational fluid dynamics," *Sci. Rep.*, vol. 15, no. 1, p. 25679, July 2025, doi: 10.1038/s41598-025-00710-2.

[11] "Olympic Ski Jumping Scoring: Distance Points, Style Marks and Wind Compensation Explained | NBC Olympics." Accessed: Oct. 08, 2025. [Online]. Available: https://www.nbcolympics.com/news/ski-jumping-101-scoring

[12] "Standard Specification for Fitness Equipment." Accessed: Oct. 08, 2025. [Online]. Available: https://store.astm.org/f2276-10r15.html

[13] "Accuracy of force sensors | Accuracy of force sensors." Accessed: Oct. 08, 2025. [Online]. Available: https://www.me-systeme.de/en/force-sensors/accuracy

[14] "Winter Climate Data," Wisconsin State Climatology Office. Accessed: Oct. 08, 2025. [Online]. Available: https://climatology.nelson.wisc.edu/wisconsin-seasons/winter/

[15] "ISO/IEC 19774-2:2019," ISO. Accessed: Oct. 08, 2025. [Online]. Available: https://www.iso.org/standard/64791.html

[16] "Standard Practice for Verification of Multi-Axis Force Measuring Platforms." Accessed: Oct. 08, 2025. [Online]. Available: https://store.astm.org/f3109-22.html

[17] O. for H. R. Protections (OHRP), "The Belmont Report." Accessed: Oct. 08, 2025. [Online]. Available: https://www.hhs.gov/ohrp/regulations-and-policy/belmont-report/index.html

[18] M. J. Field, R. E. Behrman, and I. of M. (US) C. on C. R. I. Children, "Regulatory Framework for Protecting Child Participants in Research," in *Ethical Conduct of Clinical Research Involving Children*, National Academies Press (US), 2004. Accessed: Oct. 08, 2025. [Online]. Available: https://www.ncbi.nlm.nih.gov/books/NBK25558/

[19] S.-P. Lin, W.-H. Sung, F.-C. Kuo, T. B. J. Kuo, and J.-J. Chen, "Impact of Center-of-Mass Acceleration on the Performance of Ultramarathon Runners," *J. Hum. Kinet.*, vol. 44, pp. 41–52, Dec. 2014, doi: 10.2478/hukin-2014-0109.

[20] T. Cudejko, K. Button, and M. Al-Amri, "Wireless pressure insoles for measuring ground reaction forces and trajectories of the centre of pressure during functional activities," *Sci. Rep.*, vol. 13, no. 1, p. 14946, Sept. 2023, doi: 10.1038/s41598-023-41622-3.

[21] A. Prakash, S. Sharma, and N. Sharma, "A compact-sized surface EMG sensor for myoelectric hand prosthesis," *Biomed. Eng. Lett.*, vol. 9, no. 4, pp. 467–479, Nov. 2019, doi: 10.1007/s13534-019-00130-y.

[22] "Capacitive vs Piezoresistive vs Piezoelectric Pressure Sensors | The Design Engineer's Guide | Avnet Abacus." Accessed: Dec. 10, 2025. [Online]. Available: https://my.avnet.com/abacus/solutions/technologies/sensors/pressure-sensors/core-technologies/capacitive-vs-piezoresistive-vs-piezoelectric/

[23] "Wearable Smart Sensing Insole : 13 Steps (with Pictures) - Instructables." Accessed: Dec. 10, 2025. [Online]. Available: https://www.instructables.com/Wearable-Smart-Sensing-Insole/

[24] "Biomechanics research in ski jumping, 1991–2006: Sports Biomechanics: Vol 7, No 1." Accessed: Dec. 10, 2025. [Online]. Available: https://www.tandfonline.com/doi/abs/10.1080/14763140701687560

[25] W. Storr, "Voltage Divider and Voltage Division," Basic Electronics Tutorials. Accessed: Dec. 10, 2025. [Online]. Available: https://www.electronics-tutorials.ws/dccircuits/voltage-divider.html

[26] "Voltage Divider Rule and Voltage Division - Electronics tutorials." Accessed: Dec. 10, 2025. [Online]. Available: https://www.electronics-tutorials.ws/dccircuits/voltage-divider.html

[27] W. Storr, "Analogue to Digital Converter (ADC) Basics," Basic Electronics Tutorials. Accessed: Dec. 10, 2025. [Online]. Available: https://www.electronics-tutorials.ws/combination/analogue-to-digital-converter.html

[28] "Newton's Third Law: Statement, Examples, and Equation." Accessed: Dec. 10, 2025. [Online]. Available: https://www.sciencefacts.net/newtons-third-law.html

[29] "Gravity," Math is Fun. Accessed: Dec. 10, 2025. [Online]. Available:
https://www.mathsisfun.com/physics/gravity.html

[30] M. Janura, L. Cabell, M. Elfmark, and F. Vaverka, "Kinematic Characteristics of the Ski Jump Inrun:
A 10-Year Longitudinal Study," *J. Appl. Biomech.*, vol. 26, no. 2, pp. 196–204, May 2010, doi:
10.1123/jab.26.2.196.

[31] M. Virmavirta, J. Perttunen, and P. V. Komi, "EMG activities and plantar pressures during ski
jumping take-off on three different sized hills," *J. Electromyogr. Kinesiol.*, vol. 11, no. 2, pp. 141–147,
Apr. 2001, doi: 10.1016/S1050-6411(00)00047-X.

Appendix A: Preliminary Design Specification

Function

Ski jumping is a highly technical and competitive sport that demands precise angular body
positioning and timing to achieve optimal performance. To assist youth athletes in improving their skills,
a ski jumping training system will collect biomechanical data during the in-run and takeoff portions of
the jump and compare it with reference data captured from more experienced jumpers. The system must
capture key biomechanical data metrics, including lower-body joint angles, torso stability, torso
orientation, and vertical ground reaction forces. Data analysis must be performed on these measurements
to identify differences between youth and experienced athletes. This analysis will provide youth ski
jumpers and their coaches with quantifiable feedback to improve technique, optimize takeoff timing, and
ultimately enhance jump performance.

Client Requirements

Dr. Azam Ahmed and Dr. Walter Block outlined the following specifications for the ski jumping training
system:

- The ski jump training system should be designed for youth athletes.

- The system must enable comparison between youth athletes and expert reference data.

- The ski jump training system must be usable at ski hills to capture realistic training conditions.

33

- A motion capture system that is capable of recording the 1-2 second in-phase to takeoff transition of the jumping phase.

- Video and data analysis software that provides athletes and coaches with clear points of improvement based on input data.

- The project budget is up to $5,000, contingent on demonstrated progress, to acquire various sensors, IMU, force insoles, and other necessary materials.

- Resources provided by the University of Wisconsin-Madison and recommended for use by the client include CAE software, BME teaching labs, ECB built-in force plates, and the ECB motion capture system.

- Human subject testing must follow consent procedures, especially for minors.

Design Requirements:

1. **Physical and Operational Characteristics:**

   a. **Performance Requirements:**

      i. The device must be capable of accurately calculating vertical ground reaction forces while withstanding a static load equal to 2.5 times the greater of 136 kg or the maximum specified user weight. The loading factor of 2.5 is based on intrinsic loading requirements for general consumer fitness recording equipment standards [1].

      ii. To optimize motion capture performance outdoors on ski hills, the system must utilize a minimum of three non-collinear markers per rigid body segment to track its six degrees of freedom (6-DOF) [2].

      iii. The data analysis and motion capture software GUI must be operated on devices with a minimum 800 MHz processor, 2 GB RAM, and 1 GB available hard disk space [3].

b. **Safety:**

    i.   All accessible areas of the training system must be free of burrs and sharp edges [1].

    ii.   All corners of the training system must be radiused or chamfered [1].

    iii.   Prior to testing the training system on youth athletes, parental permission and child assent must be obtained and comply with federal regulations (45 CFR 46 Subpart D) [4].

    iv.   IRB approval and oversight are required prior to human subject data collection from various ski jumping athletes: all investigators must complete certified human-subjects training [4].

    v.   Safety and injury prevention of participants must be prioritized by placing low-risk simulated practice tasks before outdoor ski hill testing [4].

c. **Accuracy and Reliability:**

    i.   The sensors in the training system must meet an accuracy class of at least 0.5, following the International Vocabulary of Metrology (VIM) standard. This ensures that the combined effects of measurement uncertainty, linearity deviation, and temperature-related drift remain within plus or minus 0.5% of full scale per 10 °C under specified operating conditions [5].

    ii.   The motion capture of our training system must measure lower-limb and torso joint angles in the sagittal plane with a precision (repeatability) better than ±3° under ski hill conditions [6].

    iii.   Under ECB teaching lab conditions, the markerless motion capture system should demonstrate relative error $\leq 0.51\%$ and absolute error $\leq 0.22°$ [6].

d. **Life in Service**

    i.   Based on ski jumping training system development guidelines, youth athletes aged 10–13 typically perform 1–2 dryland training sessions per week. The

training system must be designed to withstand this frequency of use over its service life [7].

    ii.   In terms of annual usage of the training system U12 athletes on average perform 300 to 400 jumps which the system should be able to withstand at least half if the athlete wants to track their data over time [7].

e. Shelf Life:

    i.   The piezoelectric sensors integrated into the force plate system must demonstrate a shelf life of 15–20 years under normal storage conditions (15–25 °C), non-corrosive environment, no excessive shock or vibration. [8].

    ii.   Motion capture cameras involved in our training system are IR cameras with an average shelf life of 5.7 to 11.4 years [9].

f. Operating Environment:

    i.   The training system must operate reliably in laboratory conditions with average temperatures ranging from 20-25 °C and a relative humidity of 30-50% [10]. The lab environment should be free of corrosive gases, particulates, and other harmful substances that may damage the system [10].

    ii.   The training system must also operate reliably in outdoor conditions, which can vary significantly due to the year-round nature of ski jumping. Operation must remain stable across typical seasonal changes, with details of extreme weather tolerances provided in Section J.

g. Ergonomics:

    i.   Any software element of the system that users will be interacting with should be user-friendly and should not require any prior knowledge or training.

    ii.   The comparison of relevant mechanics and metrics done by the system should be a streamlined process, and suggested improvements should be easy to understand.

iii.   The recording system should be low in component number and should follow an easy set up procedure for ease of use on the ski hill.

h.   **Size:**

i.   Components of the system must be transported up and down the ski hill as well as between the ski hill and campus and therefore should assume a relatively small size for easy transportation. Packed together, the overall system should not exceed a 0.56 m x 0.36 m x 0.23 m (22 in x 14 in x 9 in) volume in any dimension [11]. The components should be small enough to fit within these dimensions per traditional backpack size recommendations given by the DHS as this will allow easy transportation of the system.

i.   **Weight:**

i.   The weight of the system should be safe to lift and light enough to carry an extended distance by any individual regardless of strength. Components of the system will need to be transported up and down the ski jump hill and should therefore be easily transportable. The system should preferably weigh less than 20% of the transporter's personal body weight in order to avoid intense strain [12]. Further, the system should not exceed a weight of 23.1 kg if it were to be carried in a backpack per NIOSH and OSHA recommendations in order to prevent extensive damage to the bones and ligaments of the back [13].

j.   **Materials:**

i.   Durable and climate-resistant materials are a necessity for the intense setting of ski jumping. The training system should consist of materials that can survive in the harsh winter conditions of Wisconsin. These conditions include 5th percentile temperatures of -23℃ (-10 ℉) [14] and 5th percentile wind speeds of 8 m/s (18 mph) [15], per the Wisconsin Climatology Office. Further, the system should be able to endure adequate levels of moisture and precipitation, including direct

external contact with both rain and snow.

ii. Components of the design in direct contact with both human subjects and users must be made of non-irritative materials and must be absent from common allergens in order to prevent complications [16]. General biocompatibility in context with usage is required for any component utilized during human subject involvement and should therefore follow ISO standard 10993 for biological evaluation of medical devices [17].

iii. The fast-paced, dynamic nature of skiing also requires materials to be able to withstand intense force. Any component of the system worn or attached to the user must be able to withstand repeated extreme inertial, drag, and compressive forces [18].

k. **Aesthetics, Appearance, and Finish:**

i. The finish of the analysis system should be clean and smooth. The system should be absent of sharp or harsh edges and all electrical wiring should be covered and separated from the outside environment [19]. The entire system should be as simple and organized as possible for ease of use, without sacrificing functionality. The system should also present a darker color to make identification of components easier in a potential white landscape of snow on the hill. The entire system should look cohesive and should carry a professional aesthetic.

2. **Product Characteristics:**

a. **Quantity:**

i. Only one ski jump launch trainer will be designed and fabricated. The entire system will be reusable and shared amongst the users. Prototyping will be a consistent iteration of the same system and testing of the system will be done to ensure the final product has consistent output and performance.

b. **Target Product Cost:**

   i. With consideration of the various components required for the system already available at the university, and an evaluation of prices for motion capture based training systems, a target cost for the project is approximately $500 [20]. This figure is a summation that includes the $50 stipend given for the project by the department as well as further monetary support that will be provided by the client if and when required.

3. **Miscellaneous:**

   a. **Standards and Specifications**

      i. The ASTM F3109-22 standard states how to verify, test, or calibrate multi-axis force platforms like force plates used in balance. It has methods to quantify error in output signals across the working surface and force ranges, and includes parameters like the Center of Pressure. The ski jump simulator falls under this standard, as we will have to run multiple tests of the force plates to create a Voltage (ADC) vs Force (Newtons) curve to show correlation between ground reaction force and quality of the ski jump. This standard is relevant because we relied on multi-axis force plates to measure ground reaction forces during the takeoff phase of flight. It also requires generating a calibration curve that shows the relationship between applied forces and voltage (ADC) output. These procedures helped ensure the force plates produce accurate, consistent, and uniform measurements across the force plate. This is crucial because the feedback that would be given from the reaction forces fully depends on the reliability and validity of the force plate measurements[21].

      ii. The ISO/IEC 19774-2:2019 standard covers motion capture and motion data

animation for humanoid models. It specifies how to represent motion capture

data in a structured way, particularly for the use of animation of articulated

characters. It ensures compatibility and reproducibility of motion data between

systems. The ski jump simulator falls under this standard because it will use the

motion capture of humanoid models to obtain data related to the biomechanics of

ski jumping. For example, data is sampled per frame and this standard defines the

frame count, frame time (time per frame) and how the total duration is computed.

This standard is relevant because by adhering to how the humanoid motion

capture data must be structured, it ensures that the motion capture data is accurate

and reproducible for biomechanical analysis. Having well standardized and well

structured motion capture data is essential for evaluating technique of a sport like

ski jumping where the body angles change rapidly [22].

b. **Customer:**

    i.   The users of this device will be youth amateur ski jumpers with the average age

        from 8 to 12 years old. They will want the data collected to be reliable and

        accurately compared to an expert's data so they know what aspects of their jump

        they must change to improve it and more closely mimic the expert.

Patient-Related Concerns:

a. For human subject research, the participants must fully understand what data is being

collected from their ski jump, what the motion capture set up involves, and how the data

will be used, stored, or shared. Since we will be working with young amateur athletes,

getting the parents informed consent is also needed [23].

b. Participants may also be concerned about the risk of harm depending on the use of the

motion capture. If it gets in the way of the ski jump, it could cause injuries. We must

ensure the motion capture equipment does not get in the way of safety gear or impact the

jumper's mobility in any way [23].

c.   Privacy and confidentiality are crucial for the motion capture data because it could potentially personally identify the jumper by video footage or biometric signatures. To ensure privacy, we should first clearly inform the participants how long the data will be kept and who can access it as well as try to de-identify the motion capture data related to each jumper who participates [23].

d.   Since there is a trainer involved who may have the Blackhawk ski club use our motion capture system for their ski jump, it is important to make sure all participants know their participation is voluntary and that just because their club may be using our system, they aren't required to have their jump data measured and collected [23].

Competition:

Automated Motion Evaluation System from Wearable Sensor Devices for Ski Jumping

i.   Researchers developed a machine learning-based system using inertial sensors to automatically evaluate ski jumping performance, capturing full-body motion data from junior athletes and comparing it to style scores from expert judges to train and test the model [24].

ii.   The system segments jumps into key phases, analyzes kinematic features, and detects style faults in accordance with official scoring rules, showing strong alignment with human judging and offering potential for more objective, mobile performance evaluation in jury-based sports [24].

iii.   A multi-step data processing pipeline was developed to extract accurate kinematic motion data from inertial sensors, including sensor-bone alignment, orientation estimation, magnetic disturbance compensation, and joint position calculation, enabling reliable segmentation of ski jumps into key phases like flight and landing [24].

iv.   Key motion features—both technical (e.g., ski angles, joint positions) and

aesthetic (e.g., stability, leg extension)—were extracted and used in a machine learning pipeline with Dynamic Time Warping to compare jumps against reference patterns, achieving high precision and recall (70–85%) in detecting style errors relative to human judge scores [24].

Theia Markerless Motion Capture Device

v. Uses 10 SONY RX02 cameras to collect data sets of ski jumping movements in a ski jumping stadium [25].

vi. Uses data collected from cameras to offer insight into performances, technique, and aerodynamics [25].

vii. Analyzes the joint angles of the hip, knee and trunk movement across the takeoff phase, aerodynamic profiles in airflow and lift/drag during flight phase, and real-world technique to give performance insights [25].

viii. User-friendly "ANALYZE" function after calibration to accelerate data processing [25].

Foot Pressure Sensors

ix. Insoles composed of 16 pressure sensors, 3 accelerometers, and 3 angular rate sensors per side [26].

x. Great for tracking volume and distribution of force during a specific action [26].

xi. Uses many internal sensors that are hooked up to a chip that communicates to its online interface through Bluetooth [26].

Bibliography

[1] "Standard Specification for Fitness Equipment." Accessed: Sept. 18, 2025. [Online]. Available: https://store.astm.org/f2276-10r15.html

[2] "Collecting Experimental Data - OpenSim Documentation - OpenSim." Accessed: Sept. 18, 2025. [Online]. Available: https://opensimconfluence.atlassian.net/wiki/spaces/OpenSim/pages/53089986/Collecting+Experimental+Data

[3] "Supported Platforms - OpenSim Documentation - OpenSim." Accessed: Sept. 18, 2025. [Online]. Available: https://opensimconfluence.atlassian.net/wiki/spaces/OpenSim/pages/53089874/Supported+Platforms

[4] M. J. Field, R. E. Behrman, and I. of M. (US) C. on C. R. I. Children, "Regulatory Framework for Protecting Child Participants in Research," in Ethical Conduct of Clinical Research Involving Children, National Academies Press (US), 2004. Accessed: Sept. 18, 2025. [Online]. Available: https://www.ncbi.nlm.nih.gov/books/NBK25558/

[5] "Accuracy of force sensors | Accuracy of force sensors." Accessed: Sept. 18, 2025. [Online]. Available: https://www.me-systeme.de/en/force-sensors/accuracy

[6] E. Janurová, M. Janura, L. Cabell, Z. Svoboda, I. Vařeka, and M. Elfmark, "Kinematic Chains in Ski Jumping In-run Posture," J. Hum. Kinet., vol. 39, pp. 67–72, Dec. 2013, doi: 10.2478/hukin-2013-0069.

[7] "Ski Jumping Training Systems 11-14-17.pdf." Accessed: Sept. 18, 2025. [Online]. Available: https://www.usskiandsnowboard.org/sites/default/files/files-resources/files/2017-11/Ski%20Jumping%20Training%20Systems%2011-14-17.pdf

[8] A. Webdell, "How long do piezoelectric sensors last?," KDPES. Accessed: Sept. 18, 2025. [Online]. Available: https://www.kdpes.co.uk/faq-items/how-long-do-piezoelectric-sensors-last/

[9] "How long do IR LEDs last on CCTV security cameras?" Accessed: Sept. 18, 2025. [Online]. Available: https://videos.cctvcamerapros.com/support/topic/how-long-do-ir-leds-last-on-cctv-security-cameras

[10] "Managing Environmental Factors and Laboratory Conditions with Sper Scientific," MSE Supplies LLC. Accessed: Sept. 18, 2025. [Online]. Available: https://www.msesupplies.com/blogs/news/managing-environmental-factors-and-laboratory-conditions-with-sper-scientific

[11] "Backpack Airplane Travel: What Are The Dimension Limits? | QuartzMountain." Accessed: Sept. 18, 2025. [Online]. Available: https://quartzmountain.org/article/what-is-an-acceptable-back-pack-dimension-for-airplane-travel

[12] S. Dockrell, C. Simms, and C. Blake, "Schoolbag weight limit: can it be defined?," J. Sch. Health, vol. 83, no. 5, pp. 368–377, May 2013, doi: 10.1111/josh.12040.

[13] "OSHA procedures for safe weight limits when manually lifting | Occupational Safety and Health Administration." Accessed: Sept. 18, 2025. [Online]. Available: https://www.osha.gov/laws-regs/standardinterpretations/2013-06-04-0

[14] "Winter Climate Data," Wisconsin State Climatology Office. Accessed: Sept. 18, 2025. [Online]. Available: https://climatology.nelson.wisc.edu/wisconsin-seasons/winter/

[15] "Wisconsin Wind Data - Madison." Accessed: Sept. 18, 2025. [Online]. Available: https://www.aos.wisc.edu/oldsco/clim-history/stations/msn/madwind.html

[16] "Contact Allergen - an overview | ScienceDirect Topics." Accessed: Sept. 18, 2025. [Online]. Available: https://www.sciencedirect.com/topics/neuroscience/contact-allergen

[17] "ISO 10993-1:2018," ISO. Accessed: Sept. 18, 2025. [Online]. Available: https://www.iso.org/standard/68936.html

[18] "Physics Of Skiing," Real World Physics Problems. Accessed: Sept. 18, 2025. [Online]. Available: https://www.real-world-physics-problems.com/physics-of-skiing.html

[19] "1910.305 - Wiring methods, components, and equipment for general use. | Occupational Safety and Health Administration." Accessed: Sept. 18, 2025. [Online]. Available: https://www.osha.gov/laws-regs/regulations/standardnumber/1910/1910.305

[20] "Motion Capture System Prices | Motion Analysis." Accessed: Sept. 18, 2025. [Online]. Available: https://www.motionanalysis.com/pricing/

[21] "Standard Practice for Verification of Multi-Axis Force Measuring Platforms." Accessed: Sept. 18, 2025. [Online]. Available: https://store.astm.org/f3109-22.html

[22] "ISO/IEC 19774-2:2019," ISO. Accessed: Sept. 18, 2025. [Online]. Available: https://www.iso.org/standard/64791.html

[23] O. for H. R. Protections (OHRP), "The Belmont Report." Accessed: Sept. 18, 2025. [Online]. Available: https://www.hhs.gov/ohrp/regulations-and-policy/belmont-report/index.html

[24] H. Brock, Y. Ohgi, and K. Seo, "Development of an Automated Motion Evaluation System from

Wearable Sensor Devices for Ski Jumping," Procedia Eng., vol. 147, pp. 694–699, Jan. 2016, doi: 10.1016/j.proeng.2016.06.248.

[25]"Capturing Ski Jumping Biomechanics with Markerless Motion Capture | Theia Markerless." Accessed: Sept. 18, 2025. [Online]. Available: https://www.theiamarkerless.com/blog/ski jumping-biomechanics-markerless-motion-capture

[26]"Sensor insoles for clinical grade mobile gait & motion analysis." Accessed: Sept. 18, 2025. [Online]. Available: https://moticon.com/

Appendix B: Expense Table

Item	Description	Manufacturer	Mft Pt#	Vendor	Vendor Cat#	Date	QTY	Cost Each	Total	Link
Motion Capture System										
Tripod with Bag	60 inch lightweight tripod with adjustable-height legs and rubber feet, compatible with smartphone adapters.	Amazon Basics	WT 354 0	Amazon	B005K P473Q	10/1/ 2025	2	$25.99	$51.98	Amazon BasicsTr ipod
Tripod Mount Adapter	Smartphone holder, vertical and horizontal mount adapters for smart phones. Pack of 2	Sharing Moment Co.	H-2 001 12	Amazon	B07S8T TH34	10/1/ 2025	2	$6.99	$13.98	Amazon Tripod Mount
Force Plate Insoles + Accelerometers										
Right Force Insole Template	TPU 3D-printed template for force plate insole made of, 18.3 cm long	N/A	N/A	UW Design Innovati on Lab	N/A	10/1 0/20 25	1	$0.72	$0.72	N/A
Right Force Insole Template	PLA 3D-printed template for force plate insole made of, 18.3 cm long	N/A	N/A	UW Design Innovati on Lab	N/A	10/1 3/20 25	1	$0.56	$0.56	N/A
Right Force Insole Template	PLA 3D-printed template for force plate insole made of, 20.8 cm long	N/A	N/A	UW Design Innovati on Lab	N/A	10/1 5/20 25	1	$0.59	$0.59	N/A
Right Force Insole Template	PLA 3D-printed template for force plate insole, dimensions 24.2 cm long	N/A	N/A	UW Design Innovati on Lab	N/A	10/1 6/20 25	1	$0.80	$0.80	N/A
Left Force Insole	PLA 3D-printed template for force plate insole, dimensions 24.2 cm long	N/A	N/A	UW Design Innovati	N/A	10/2 2/20 25	1	$0.80	$0.80	N/A

				on Lab						
Electrical Tape	SWRT 6 Pack Black Electrical Tape 0.75in x 66ft 600V	SWRT	N/A	Adafruit	B0DLNGHJZH	10/20/2025	1	$7.99	$7.99	Amazon ElectricalTape
Copper Tape	Copper foil tape with conductive adhesive 6mm x 15	Adafruit	1128	Adafruit	1128	10/16/2025	1	$5.95	$5.95	Copper Tape
Velostat Sheet	Pressure-Sensitive Conductive Sheet 28cm x 28cm	Adafruit	1361	Adafruit	1361	10/16/2025	2	$4.95	$9.90	Velostat
Accelerometers	ISM330DHCX - 6 DOF IMU - Accelerometer and Gyroscope	Adafruit	4502	Adafruit	4502	10/16/2025	3	$19.95	$59.85	Proto-board
ESP32	Adafruit ESP32 Feather Wifi + BT microcontroller	Adafruit	5400	Adafruit	5400	10/22/2025	3	$19.95	$59.85	ESP32
LIPO Battery	Lithium Ion Polymer Battery - 3.7V 2500mAh	Adafruit	328	Adafruit	328	10/22/2025	3	$14.95	$14.95	LIPOBattery
Proto-Board	PCB Proto-Board 4cm x 6cm 3-pack	Adafruit	4785	Adafruit	4785	10/22/2025	2	$2.50	$5.00	Proto-Board
Women's Right Force Insole Templates	PLA 3D-printed template for force plate insole, dimensions: 24.2x8x0.1 cm	N/A	N/A	UW Design Innovation Lab	N/A	10/31/2025	2	$0.54	$1.08	N/A
Women's Left Force Insole Templates	PLA 3D-printed template for force plate insole, dimensions: 24.2x8x0.1 cm	N/A	N/A	UW Design Innovation Lab	N/A	10/31/2025	2	$0.54	$1.08	N/A
Men's Right Force Insole Templates	PLA 3D-printed template for force plate insole, dimensions: 22.9x7.5x0.1 cm	N/A	N/A	UW Design Innovation Lab	N/A	10/31/2025	2	$0.46	$0.92	N/A
Men's Left Force Insole Templates	PLA 3D-printed template for force plate insole, dimensions: 22.9x7.5x0.1 cm	N/A	N/A	UW Design Innovation Lab	N/A	10/31/2025	2	$0.46	$0.92	N/A
Housing Unit	PLA 3D-printed housing unit for microcontroller + lid	N/A	N/A	UW Design Innovation Lab	N/A	11/18/2025	1	$0.99	$0.99	N/A
Power Straps	Pack of 2 power straps for	ZipFit	N/A	ZipFit	N/A	11/1	1	$40.00	$40.00	ZipFitP

	ski boots to attach the housing unit to the jumper's boot					9/20 25				owerStr aps
Microcontroller storage unit + lid V1.	PLA 3D-printed box + lid	N/A	N/A	UW Design Innovati on Lab	N/A	11/1 8/20 25	1	$0.99	$0.99	N/A
Microcontroller storage unit + lid V2.	PLA 3D-printed box + lid	N/A	N/A	UW Design Innovati on Lab	N/A	11/2 0/20 25	1	$1.19	$1.19	N/A
Microcontroller storage unit + lid V2.	PLA 3D-printed box + lid	N/A	N/A	UW Design Innovati on Lab	N/A	12/1/ 2025	1	$1.19	$1.19	N/A
								TOTAL:	**$281.28**	

Appendix C: Arduino IDE Project Code

```
#include <WiFi.h>
#include <Wire.h>
#include <Adafruit_Sensor.h>
#include <Adafruit_ISM330DHCX.h>

const char webpage[] PROGMEM = R"rawliteral(
<!DOCTYPE html>
<html>
<head>
<title>Ski Jump Data Dashboard</title>
<meta name="viewport" content="width=device-width, initial-scale=1">

<style>
body { font-family: Arial; background:#f0f2f5; margin:0; padding:10px; }
h1 { text-align:center; font-weight:bold; }

.card {
   background:white; padding:15px; margin-bottom:20px;
   border-radius:12px; box-shadow:0 3px 10px rgba(0,0,0,0.1);
}
.label { font-size:16px; font-weight:bold; }
.value { font-size:20px; color:#0077cc; }
```

46

```
</style>

</head>
<body>

<h1>ESP32 Live Sensor Dashboard</h1>

<!-- Cube placeholder so JS doesn't break -->
<div id="cube" style="width:50px; height:50px; background:#ccc; margin:auto;"></div>

<div class="card">
   <div class="label">Accel X:</div><div id="ax" class="value">--</div>
   <div class="label">Accel Y:</div><div id="ay" class="value">--</div>
   <div class="label">Accel Z:</div><div id="az" class="value">--</div>
</div>

<div class="card">
   <div class="label">Back Pressure:</div><div id="p1" class="value">--</div>
   <div class="label">Front Pressure:</div><div id="p5" class="value">--</div>
</div>

<canvas id="accelCanvas" width="350" height="150"></canvas>
<canvas id="pressureCanvas" width="350" height="150"></canvas>

<script>
// === Live update function ===
function updateData() {
   fetch("/data")
     .then(r => r.json())
     .then(d => {
        document.getElementById("ax").innerHTML = d.ax.toFixed(2);
        document.getElementById("ay").innerHTML = d.ay.toFixed(2);
        document.getElementById("az").innerHTML = d.az.toFixed(2);

        document.getElementById("p1").innerHTML = d.p1.toFixed(2);
        document.getElementById("p5").innerHTML = d.p5.toFixed(2);
     });
}

// update 4×/sec
setInterval(updateData, 250);
</script>

</body>
```

```
</html>
)rawliteral";

// WiFi Access Point credentials
const char* ssid = "ESP32SkiJumping";
const char* password = "FadingFootball";

WiFiServer server(80);
Adafruit_ISM330DHCX ism;

// ADC pins for analog inputs
const int pinBack  = 34;
//const int pinLeft  = 25;
//const int pinRight = 39;
const int pinFront = 36;

void setup() {
  Serial.begin(115200);

  // Start WiFi AP
  WiFi.softAP(ssid, password);
  Serial.print("Access Point IP: ");
  Serial.println(WiFi.softAPIP());

  server.begin();

  // Initialize accelerometer
  if (!ism.begin_I2C()) {
    Serial.println("Failed to find ISM330DHCX chip");
    while (1) { delay(10); }
  }
}

void loop() {
  WiFiClient client = server.available();
  if (!client) return;

  // Wait for request
  while (!client.available()) delay(1);
  String req = client.readStringUntil('\r');
  client.flush();

  // --- JSON data endpoint ---
  if (req.indexOf("GET /data") >= 0) {
```

```
   sensors_event_t accel, gyro, temp;
   ism.getEvent(&accel, &gyro, &temp);

   int rawBack  = analogRead(pinBack);
 //  int rawLeft  = analogRead(pinLeft);
   //int rawRight = analogRead(pinRight);
   int rawFront = analogRead(pinFront);

   float back  = rawBack  * (3.3 / 4095.0);
  // float left  = rawLeft  * (3.3 / 4095.0);
   //float right = rawRight * (3.3 / 4095.0);
   float front = rawFront * (3.3 / 4095.0);

   client.println("HTTP/1.1 200 OK");
   client.println("Content-Type: application/json");
   client.println("Connection: close");
   client.println();
   client.print("{");
   client.print("\"ax\":"); client.print((accel.acceleration.x) - 1.48); client.print(",");
   client.print("\"ay\":"); client.print((accel.acceleration.y) - 5.80); client.print(",");
   client.print("\"az\":"); client.print((accel.acceleration.z) - 7.67); client.print(",");
   client.print("\"gz\":"); client.print(gyro.gyro.z); client.print(",");
   client.print("\"p1\":"); client.print(back); client.print(",");
   //client.print("\"p3\":"); client.print(left); client.print(",");
   //client.print("\"p4\":"); client.print(right); client.print(",");
   client.print("\"p5\":"); client.print(front);
   client.println("}");
 }
 // --- HTML page ---
 else {
  client.println("HTTP/1.1 200 OK");
 client.println("Content-Type: text/html");
 client.println("Content-Encoding: none");
 client.println("Connection: close");
 client.println();
 client.write_P(webpage, strlen_P(webpage));   // <-- serves big dashboard
}
}
```

Appendix D: Housing Unit Fabrication Protocol

1. Open Onshape and create a new document to make part

1. Create a new sketch on the Top plane and draw a 3.346 inches by 2.559 inches rectangle.

2. Extrude rectangle up 1.279 inches.

3. Create a new sketch on the top plane of the box and draw a center point rectangle 2.756 inches by 1.969 inches.

4. Extrude down into the box 1.1811 inches.

5. Create a new sketch on the right face of the box and draw a center point rectangle 1.969 inches by 0.394 inches.

6. Extrude rectangle from prior step 0.394 inches and duplicate it on the left side of the box.

7. Once both handles are extruded, create a new sketch and draw a rectangle from where the handle connects to the box to 0.275 inches across the handle. Set the length of this rectangle to 1.6 inches. Repeat on the other handle.

8. Extrude through the rectangles in the previous step to create the handles.

9. Create a new sketch on the front face of the box. Sketch a rectangle on the center of that face for the button 0.416 inches by 0.228 inches. Sketch another rectangle for the wire hole at the center of the right half of the front face 0.591 inches by 0.295 inches.

10. Extrude through the two rectangles in the previous step all the way through to create the button hole and the wire hole.

11. Filet all the edges of the box with a 0.079 inch radius.

12. Face blends the interior faces of the handles with a 0.2 inch radius.

13. Create a new sketch and draw circles for screw holes 3/32 in diameter and place them 0.204 inches away from the corner of the filet.

14. Extrude down into the hole sketches 1 inch deep.

15. Create a lid 0.098 inches thick with holes 0.204 inches away from the corners diagonally. The diameter of the holes should be 3/32 inches.

16. Save both files in stl. Format for 3D printing.

17. Print at Wendt and allow print to complete.

18. Remove the housing unit from the print bed carefully and clean up any support material using a small blade or file.

19. Make small step-wise adjustments to the fit or openings if necessary.

20. Drill an LED hole on the front face using a drill bit

Appendix E: Force Insole Fabrication Protocol

Step-by-Step Protocol

1. 3D Print force insole template with 1 mm thickness in PLA

2. Apply copper tape along the designated traces on the insole. Tape traces must not touch each other and extra tape at the sensor locations can be folded back on itself.

3. Cut the Velostat sheet into small elliptical pieces and secure each piece in place on the template using electrical tape. Make sure that the layer of the electrical tape placed prior, is in direct and secure contact with the bottom of the Velostat piece. Sensors must not touch one another or any neighboring traces.

4. Solder thin gauge wire directly to the copper tape at the heel of the insole, ensuring the wires are long enough to reach out of the boot and into the housing unit prior to soldering. Apply a layer electrical tape over the soldered connection to insulate and secure the junction.

5. Further secure the Velostat and copper tape by placing ample electrical tape along the insole.

6. Then put copper wire over the top of the tape making sure copper tape makes contact with the sensor and it extends to the heel. Solder a single cable at the heel long enough to reach the micro-controller.

7. Solder the other ends of the wires coming from the insole to the appropriate locations on the ESP32, specifically the beginning of the 10 Kohm resistors where the Vout wire originates.

Appendix F: Force Insole CSV to Graph MATLAB Code + Data Table

```
%% Select your athlete's data file
% Choose the CSV file you downloaded from the insoles.

close all;
clear all;
[file, path] = uigetfile('*','Select the file to open');
raw = importdata([path, filesep, file]);

%% Convert time into seconds
```

% The time column is in milliseconds; this changes it to seconds
% and starts the clock at 0.

time_ms = raw.data(:,1);
time_s = (time_ms - time_ms(1)) / 1000;

%%% Load heel and forefoot force data
% These columns represent force under the heel and forefoot.

p1_back = raw.data(:,5);   % Heel
p5_front = raw.data(:,6);   % Forefoot

%%% Clean the force signal
% Uses the start of the recording to remove baseline noise
% and flips the signal so force increases upward on the graph.

nBaseline = min(100, length(p1_back));
p1_inverted = -(p1_back - mean(p1_back(1:nBaseline)));   % Heel
p5_inverted = -(p5_front - mean(p5_front(1:nBaseline))); % Forefoot

%%% Find the peak forces
% Identifies the highest force for both heel and forefoot.

[peakHeel,idxHeel] = max(p1_inverted);
[peakForefoot,idxForefoot] = max(p5_inverted);

timeHeelPeak = time_s(idxHeel);
timeForePeak = time_s(idxForefoot);

%%% Plot the force curves
% Displays force over time for heel and forefoot.

figure;
hold on;
plot(time_s, p1_inverted, 'LineWidth', 1.5);
plot(time_s, p5_inverted, 'LineWidth', 1.5);

%%% Mark the peak points on the graph
% Adds marker to show where the max forces occurred.

plot(timeHeelPeak, peakHeel, 'o', 'MarkerSize', 5, 'MarkerFaceColor', 'k');
plot(timeForePeak, peakForefoot, 'o', 'MarkerSize', 5, 'MarkerFaceColor', 'k');

%%% Label the peak force values

% Displays the numeric value of each peak on the graph.

text(timeHeelPeak, peakHeel, ...
   sprintf(' Heel Peak: %.0f N', peakHeel), ...
   'VerticalAlignment', 'bottom');

text(timeForePeak, peakForefoot, ...
   sprintf(' Forefoot Peak: %.0f N', peakForefoot), ...
   'VerticalAlignment', 'bottom');

%% Add graph labels
% Makes the graph easier to understand.

legend('Heel', 'Forefoot', 'Location', 'best');
title("Force vs. Time: Front and Back Sensors");
xlabel("Time (s)");
ylabel("Vertical Ground Reaction Force (N)");
grid on;

Dynamic Jump Table

Trial	Averaged ADC - Force Insoles	Force N - Force Plate
1 (light)	**2300, 3251 ADC**	**1029.546 N**
2 (light)	**2050, 3459 ADC**	**1403.28 N**
3 (light)	**2280, 3312 ADC**	**1222.623 N**
4 (light)	**2350 , 3251 ADC**	**1087.32 N**
5 (light)	**2400, 3251 ADC**	**1042.253 N**
6 (light)	**2000, 3453 ADC**	**1283.019 N**
7 (light)	**2000, 3340 ADC**	**1236.876 N**
8 (medium)	**2350, 3798 ADC**	**1345.387 N**

9 (medium)	2700, 3910 ADC	1440.034 N
10 (medium)	2400, 3451 ADC	1363.163 N
11 (medium)	2280, 3514 ADC	1414.77 N
12 (medium)	2160, 3539 ADC	1342.584 N
13 (medium)	2150, 3583 ADC	1251.369 N
14 (medium)	2200, 3673 ADC	1347.243 N
15 (heavy)	2200, 3565 ADC	1542.276 N
16 (heavy)	2100, 3940 ADC	1555.909 N
17 (heavy)	1900, 3631 ADC	1897.91 N
18 (heavy)	2000, 3631 ADC	1912.175 N
19 (heavy)	2150, 3632 ADC	1998.434 N
20 (heavy)	2000, 3631 ADC	1940.248 N
21 (heavy)	2000, 3439 ADC	1816.952 N

ADC to Voltage Equation

Vout = (ADC/4096) *3.3

Voltage to Resistance Equation

$$V_{\text{out}} = V_{\text{in}} \cdot \frac{R_{\text{fixed}}}{R_{\text{vel}} + R_{\text{fixed}}}$$

$$R_{\mathrm{vel}} = R_{\mathrm{fixed}} \cdot \frac{V_{\mathrm{in}} - V_{\mathrm{out}}}{V_{\mathrm{out}}} = 10{,}000 \cdot \frac{3.3 - V_{\mathrm{out}}}{V_{\mathrm{out}}}$$

Appendix G: Kinovea Angle Graph Analysis Code

```
%% Kinovea Data Graph of USA and Green/Black Ski Jumpers
close all;   % closes all open figures each time you run
clear all;
% Read in data for both ski jumpers
usa28 = readtable("/Users/ks14/Library/Mobile Documents/com~apple~CloudDocs/UW 25:26/BME
design/usa28.knee.ankle.data.csv");
usa30 = readtable("/Users/ks14/Library/Mobile Documents/com~apple~CloudDocs/UW 25:26/BME
design/usa30.ankle.knee.data.csv");
usa36 = readtable("/Users/ks14/Library/Mobile Documents/com~apple~CloudDocs/UW 25:26/BME
design/usa36.knee.angle.data.csv");
usa40 = readtable("/Users/ks14/Library/Mobile Documents/com~apple~CloudDocs/UW 25:26/BME
design/usa40.knee.ankle.data.csv");
bg29 = readtable("/Users/ks14/Library/Mobile Documents/com~apple~CloudDocs/UW 25:26/BME
design/greenblack29.knee.ankle.data.csv");
bg33 = readtable("/Users/ks14/Library/Mobile Documents/com~apple~CloudDocs/UW 25:26/BME
design/greenblack33.knee.angle.data.csv");
bg37 = readtable("/Users/ks14/Library/Mobile Documents/com~apple~CloudDocs/UW 25:26/BME
design/greenblack37.knee.angle.data.csv");
bg41 = readtable("/Users/ks14/Library/Mobile Documents/com~apple~CloudDocs/UW 25:26/BME
design/greenblack41.knee.ankle.data.csv");

%% USA Jumper (converted to vectors)
usa28_time       = usa28{:, "Time_ms_"};
usa28_knee_angle  = usa28{:, "KneeAngle"};
usa28_ankle_angle = usa28{:, "AnkleAngle"};

usa30_time       = usa30{:, "Time_ms_"};
usa30_knee_angle  = usa30{:, "KneeAngle"};
usa30_ankle_angle = usa30{:, "AnkleAngle"};

usa36_time       = usa36{:, "Time_ms_"};
usa36_knee_angle  = usa36{:, "KneeAngle"};
usa36_ankle_angle = usa36{:, "AnkleAngle"};
```

```matlab
usa40_time       = usa40{:, "Time_ms_"};
usa40_knee_angle  = usa40{:, "KneeAngle"};
usa40_ankle_angle = usa40{:, "AnkleAngle"};


%%% Green/Black Jumper (converted to vectors)
bg29_time        = bg29{:, "Time_ms_"};
bg29_knee_angle  = bg29{:, "KneeAngle"};
bg29_ankle_angle = bg29{:, "AnkleAngle"};


bg33_time        = bg33{:, "Time_ms_"};
bg33_knee_angle  = bg33{:, "KneeAngle"};
bg33_ankle_angle = bg33{:, "AnkleAngle"};


bg37_time        = bg37{:, "Time_ms_"};
bg37_knee_angle  = bg37{:, "KneeAngle"};
bg37_ankle_angle = bg37{:, "AnkleAngle"};


bg41_time        = bg41{:, "Time_ms_"};
bg41_knee_angle  = bg41{:, "KneeAngle"};
bg41_ankle_angle = bg41{:, "AnkleAngle"};


%%% Convert USA time vectors to seconds
usa28_time = usa28_time / 1000;
usa30_time = usa30_time / 1000;
usa36_time = usa36_time / 1000;
usa40_time = usa40_time / 1000;


%%% Convert Green/Black time vectors to seconds
bg29_time = bg29_time / 1000;
bg33_time = bg33_time / 1000;
bg37_time = bg37_time / 1000;
bg41_time = bg41_time / 1000;


%%% Zero the time values for each jump
usa28_time = usa28_time - usa28_time(1);
usa30_time = usa30_time - usa30_time(1);
usa36_time = usa36_time - usa36_time(1);
usa40_time = usa40_time - usa40_time(1);


bg29_time  = bg29_time  - bg29_time(1);
bg33_time  = bg33_time  - bg33_time(1);
bg37_time  = bg37_time  - bg37_time(1);
```

```matlab
bg41_time  = bg41_time  - bg41_time(1);

%% ---- USA Knee Angle Plot ----
figure(1)
subplot(2,1,1);     % 2 rows, 1 column, top plot
hold on
plot(usa28_time, usa28_knee_angle);
plot(usa30_time, usa30_knee_angle);
plot(usa36_time, usa36_knee_angle);
plot(usa40_time, usa40_knee_angle);

title("Ski Jumper 1: Knee Angle vs Time");
xlabel("Time (s)");
ylabel("Knee Angle (Deg)");
grid on
legend("USA28", "USA30", "USA36", "USA40");
hold off

%% ---- USA Ankle Angle Plot ----
subplot(2,1,2);     % 2 rows, 1 column, bottom plot
hold on
plot(usa28_time, usa28_ankle_angle);
plot(usa30_time, usa30_ankle_angle);
plot(usa36_time, usa36_ankle_angle);
plot(usa40_time, usa40_ankle_angle);


title("Ski Jumper 1: Ankle Angle vs Time");
xlabel("Time (s)");
ylabel("Ankle Angle (Deg)");
grid on
legend("USA28", "USA30", "USA36", "USA40");
hold off

%% ---- Green/Black Knee Angle Plot ----
figure(2)   % New figure for Green/Black group

subplot(2,1,1);     % Top plot
hold on
plot(bg29_time, bg29_knee_angle);
plot(bg33_time, bg33_knee_angle);
plot(bg37_time, bg37_knee_angle);
plot(bg41_time, bg41_knee_angle);
```

```
title("Ski Jumper 2: Knee Angle vs Time");
xlabel("Time (s)");
ylabel("Knee Angle (Deg)");
grid on
legend("GB29", "GB33", "GB37","GB41");
hold off

%% ---- Green/Black Ankle Angle Plot ----
subplot(2,1,2);     % Bottom plot
hold on
plot(bg29_time, bg29_ankle_angle);
plot(bg33_time, bg33_ankle_angle);
plot(bg37_time, bg37_ankle_angle);
plot(bg41_time, bg41_ankle_angle);


title("Ski Jumper 2: Knee Angle vs Time");
xlabel("Time (s)");
ylabel("Ankle Angle (Deg)");
grid on
legend("GB29", "GB33", "GB37","GB41");
hold off
```